Chapter 7
Combined Approaches to Study Virus Structures

Daniel Badia-Martinez, Hanna M. Oksanen, David I. Stuart, and Nicola G.A. Abrescia

Abstract A virus particle must work as a safe box for protecting its genome, but at the same time it has to undergo dramatic conformational changes in order to preserve itself by propagating in a cell infection. Thus, viruses are miniaturized wonders whose structural complexity requires them to be investigated by a combination of different techniques that can tackle both static and dynamic processes. In this chapter we will illustrate how major structural techniques such as X-ray crystallography and electron microscopy have been and can be combined with other techniques to determine the structure of complex viruses. The power of these hybrid method approaches are revealed through the various examples provided.

Keywords Hybrid methods • X-ray crystallography • Electron microscopy • Cryo-electron microscopy • Electron tomography • Cryo-electron tomography • Small-angle X-ray scattering • Virus • Bacteriophage • Capsid • Mutagenesis • Dissociation • Crystal structure • Fitting

D. Badia-Martinez
Structural Biology Unit, CICbioGUNE, CIBERehd, Bizkaia Technology Park, 48160 Derio, Spain

H.M. Oksanen
Institute of Biotechnology and Department of Biosciences, Viikki Biocenter, University of Helsinki, P.O. Box 56, Viikinkaari 5, 00014 Helsinki, Finland

D.I. Stuart
Division of Structural Biology, The Wellcome Trust Centre for Human Genetics, University of Oxford, Roosevelt Drive, Headington, Oxford OX3 7BN, UK

Diamond Light Source Ltd, Diamond House, Harwell Science and Innovation Campus, Didcot, UK

N.G.A. Abrescia (✉)
Structural Biology Unit, CICbioGUNE, CIBERehd, Bizkaia Technology Park, 48160 Derio, Spain

Ikerbasque, Basque Foundation for Science, 48011 Bilbao, Spain
e-mail: nabrescia@cicbiogune.es

M.G. Mateu (ed.), *Structure and Physics of Viruses: An Integrated Textbook*, Subcellular Biochemistry 68, DOI 10.1007/978-94-007-6552-8_7,

Abbreviations

2D	Two dimensional
3D	Three dimensional
BMV	Bromegrass mosaic virus
EM	Electron microscopy
ET	Electron tomography
Fab	Antigen-binding antibody fragment
FMDV	Foot-and-mouth disease virus
HCV	Hepatitis C virus
HCV-LP	HCV-like particle
HIV	Human immunodeficiency virus
HRV-16	Human rhinovirus 16
HSV	Herpes simplex virus
MR	Molecular replacement
NCS	Non-crystallographic symmetry
NMR	Nuclear magnetic resonance
RVFV	Rift Valley fever virus
SANS	Small-angle neutron scattering
SAXS	Small-angle X-ray scattering
SBMV	Southern bean mosaic virus
SeMet	Seleno-methionine
SIV	Simian immunodeficiency virus
TBSV	Tomato bushy stunt virus
TEM	Transmission electron microscopy
TMV	Tobacco mosaic virus
TNV	Tobacco necrosis virus
VLP	Virus-like particle
WNV	West Nile virus

7.1 Introduction: The 'Multi-Disciplinary Approach' Concept in Structural Virology

7.1.1 Early Structural Studies on Viruses

In previous chapters several independent approaches to study virus structure including electron microscopy (EM, Chap. 3), X-ray crystallography (Chap. 4), nuclear magnetic resonance spectroscopy (NMR, Chap. 5), mass spectrometry (MS) and other spectroscopic methods (Chap. 6) have been described. In this chapter, we will illustrate how some of those methods can be combined to provide further insights into virus structures. To clarify how these initially independent methods have converged, complemented and combined with each

other in the study of viruses, we will provide a brief historical perspective and a recapitulation of some of these structural methods as applied to virology (Fig. 7.1).

Structural virology began when Ernst Ruska built the first electron microscope and together with his brother, medical doctor, Helmut Ruska initiated the imaging of viruses and other submicroscopic structures during the years 1938 and 1939. Alongside this, the principles for the small-angle X-ray scattering (diffraction) (SAXS) technique were proposed by André Guinier (see Sect. 7.2.2). In 1935, Wendell Stanley provided the conditions for crystallization of the first virus, the tobacco mosaic virus (TMV), a plant-infecting virus. For his studies in producing pure enzymes and viruses, in 1946 he was awarded with the Nobel Prize in Chemistry. Also Ruska received the Nobel Prize but in Physics for his fundamental contribution in electron optics, incredibly, 55 years after building of his first microscope! In 1937, Bawden and Pirie crystallized another plant virus, tomato bushy stunt virus (TBSV) but it wasn't until 1941 that crystals of TBSV and TMV produced clear X-ray diffraction patterns.

The 1950s saw the beginning of the modern biology with the determination of the three-dimensional (3D) structure of the DNA by James Watson and Francis Crick and the first high-resolution X-ray structures of proteins, myoglobin by John Kendrew and hemoglobin by Max Perutz. Interestingly, in 1956 Watson and Crick also proposed the principles of virus organization. According to their hypothesis based on electron micrographs of plant viruses and their propensity to form crystals and concepts of genetic economy, simple viruses were formed by capsid of multiple copies of relatively small proteins arranged in a symmetrical fashion, providing identical protein contacts among their neighbours. They suggested that a cubic symmetry or a cylindrical shell would satisfy the above requirements whilst allowing a larger volume of nucleic acid to be packaged. The case for icosahedral symmetry of viruses was made by John Finch and Aaron Klug in 1959 in unveiling the organisation of poliomyelitis virus by X-ray diffraction in 1959. Caspar and Klug continued on this idea and formulated the quasi-equivalence theory indicating that certain multiples of 60 subunits could also form viral capsids but the equivalent interactions among neighbour subunits could no longer exist. Klug's thinking on this was inspired by the work of Buckminster Fuller in particular by his book *The Dymaxion World of Buckminster Fuller*. Caspar and Klug based the quasi-equivalent theory on the fact that the capsomers are adaptable molecules that organize in different ways within a highly ordered structure thus introducing the concept of protein flexibility to explain these different arrangements (see Chap. 2). Methods development for 3D reconstruction from electron micrographs began in 1964 when Aaron Klug and Jacob Berger introduced the use of Fourier transform in micrograph analysis. This analysis was extended to object with rotational symmetry, helical symmetry (for rod-shaped viruses) and finally to icosahedral specimens (for an historical account see 'Further reading' at the end of this chapter). In the same period Walter Hoppe, who contributed to the development of methods and instrumentation in X-ray analysis moved to the electron microscopy field transferring the same momentum and know-how in the advances of electron microscopy methods (see the ptychography technique in Sect. 7.7.2).

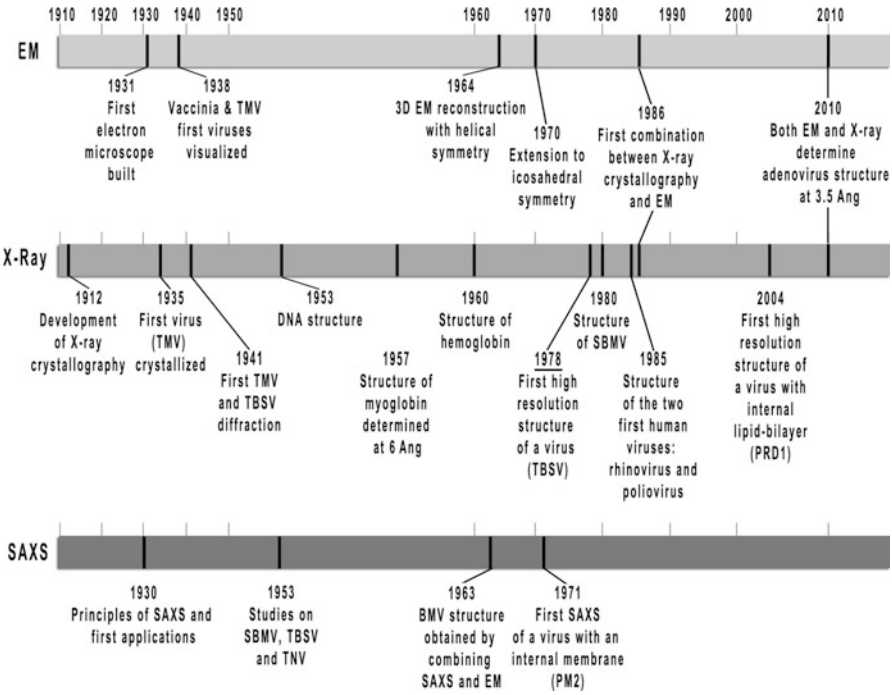

Fig. 7.1 Timeline of the major achievements in structural virology by EM, X-ray crystallography and SAXS techniques for the determination of virus structures. Due to their relevance the DNA and myo-hemoglobin structures have been included. Tobacco mosaic virus (*TMV*); Tobacco necrosis virus (*TNV*); tomato bushy stunt virus (*TBSV*); lipid-containing bacteriophage PRD1 (*PRD1*); southern bean mosaic virus (*SBMV*); bromegrass mosaic virus (*BMV*); lipid-containing bacteriophage PM2 (*PM2*)

Together with X-ray and EM, also small-angle scattering (using both X-rays [SAXS], and neutrons, [small-angle neutron scattering, or SANS]) was contributing to the analysis of virus structures. However in the years that followed, the impact of SAXS as a primary method became weaker leaving the leading role in structural virology to the other two structural techniques (Fig. 7.1). In parallel to the above developments, efforts were made to improve the diffraction of virus crystals and to devise ways to analyse symmetric structures that ultimately culminated into the structure of TBSV at 2.9-Å resolution in 1978 [1] and two years later into the structure of southern bean mosaic virus (SBMV) at 2.8-Å resolution [2]. Since then, both virus crystallography and electron microscopy have been fundamental techniques in providing structural insights in complex viruses. The techniques are complementary and well suited to hybridisation.

7.1.2 The Emerging Concept of Hybrid Methods

To grasp the concept of hybrid methods in structural virology one has to go back to the early culture of structural biology. The methods were developed to answer

fundamental biological questions but the X-ray diffractometers and microscopes were designed, built and maintained by engineers, physicists and biophysicists. The interdisciplinary expertises gathered in pioneering laboratories, in, among others, Birbeck and King's College in London (JD Bernal and Rosalind Franklin), Oxford University (Dorothy Hodgkin), the Royal Institution London (Lawrence Bragg and David Phillips) and the MRC Unit for the Study of the Molecular Structure of Biological Systems at Cambridge University (Max Perutz) around the middle of the twentieth century forged the spirit and the ambition to tackle the unexplored complexity of biology by complementary approaches (see Max Perutz's video interview and commentary on: http://www.youtube.com/watch?v=5I4eq63-3_I).

Thus, from one side, complex biological systems were reduced to smaller pieces (proteins or protein domains), in a reductionist (or "top-to-bottom") approach, studied separately and then, possibly, put back again in an overall framework (see also Chap. 5 regarding this approach in virus structure studies using NMR). On the other side, the complexity of larger macromolecular assemblies such as viruses could be looked at head-on thanks to the diverse expertise in those laboratories. So, hybrid methods and expertises were from the start supporting each other, validating the results obtained by the individual techniques.

Over the past three decades the multi-disciplinary approach has moved on from its original rationale towards the use of hybrid methods in predicting biological interactions, in uncovering dynamic processes and in bridging different resolution scales in molecular and cellular processes. The study of human adenovirus, a complex non-membrane icosahedral dsDNA virus (see below and Chap. 11) provides a good example of this. Indeed, this is the first case of combining X-ray crystallography and electron microscopy data, where the crystal structure of the viral capsid protein, assembled as stable capsomeric hexamers (hexons), was used to build an atomic model of the entire virion by exploiting the capsomer arrangement revealed by electron microscopy [3]. Since then the individual methods have become more powerful and the combination of (cryo-)EM and X-ray crystallography is a method of choice not just for many viruses but generally within structural biology.

In this chapter we will focus on describing how hybrid methods, with emphasis on the combination of X-ray crystallography and EM, have shaped our understanding of virus structures. We will provide examples of their contributions to the structure solution of very large and complex viruses and briefly discuss the challenges ahead, highlighting the power and vigour of methodological interactions in structural virology.

7.2 Some Classical Methods in Structural Virology: A Brief Overview

In this section we will recapitulate the three major structural techniques that have primarily contributed to the understanding of virus structures: EM, SAXS/SANS and X-ray crystallography. EM and X-ray crystallography as applied to viruses have been described extensively in Chaps. 3 and 4, respectively. Here we simply underline those concepts that link the methods.

7.2.1 Electron Microscopy

Transmission electron microscopy (TEM) relies on an electron beam passing through a virus sample either negatively stained to enhance the contrast or (in cryo-EM) vitrified at <100 K to ameliorate the radiation damage (vitrification is usually through simple flash freezing, but freezing rates may be enhanced by a simultaneous pressure wave; see Chap. 3). Electrons scattered elastically *via* the Coulomb potential of the atoms composing the virus (or any biological/material sample) are combined *via* magnetic lenses to generate a magnified image of the specimen. Depending on the TEM set-up data can be recorded in real space (images) or a reciprocal space (diffraction). In mathematical terms what allows the scattering process to be formalized in one or the other space is the Fourier transform (see also Chaps. 3 and 4). Since the energy of the electrons is very high their equivalent wavelength is much shorter than that for the X-rays used in crystallography. As a consequence in the case of image-mode, the result is a two-dimensional (2D) projection (real space) conceptually equivalent to the optical image obtained by cameras and visible light microscopes. In reciprocal space this corresponds to a plane of information which passes through the origin of reciprocal space (a central section) and information on both amplitude and phase of the transform of the elastically scattered electrons can be derived (Fig. 7.2). In the diffraction-mode only the amplitudes can be directly calculated from the measured intensity of diffraction spots (reciprocal space) but with higher precision and resolution than the corresponding values extracted from real-space images, which provide the less precise phase information (Fig. 7.2).

The dual-use of TEM in image- and diffraction- modes on the same sample constitutes the field of 2D electron crystallography. However, to collect electron diffraction images it is fundamental that the specimen forms a 2D ordered lattice, a requirement not needed for imaging mode. By combining these modes, 2D-electron crystallography circumvents the 'phase-problem' that X-ray crystallography must inevitably face (see Chap. 4). Each EM snapshot is equivalent to a 'still' X-ray image. Interestingly, it has proved much easier to generate 3D crystals than 2D (perhaps especially so for viruses which are often isometric), so the field of 2D crystallography remains much less developed.

Viruses have been investigated by EM since its early days due to their large and regular shape and relative ease of purification. Indeed, since the visualization of the first viruses in 1938–39 [4], a head-to-head race began in the technological advances of each of the major structural techniques at the time: EM, SAXS and X-ray crystallography (Figs. 7.1 and 7.2). Electron microscopy remains a workhorse method in several different aspects of virology from virus detection and identification to the 3D structure determination and analysis of virus-cell interactions. Continuing developments mean that nowadays electron microscopy can provide near-atomic resolution structures of viruses where atoms though not resolved, can be inferred [5] (see Chap. 3). The highest resolution analyses come from combining many projections of the virion collected from different particles thrown down at random;

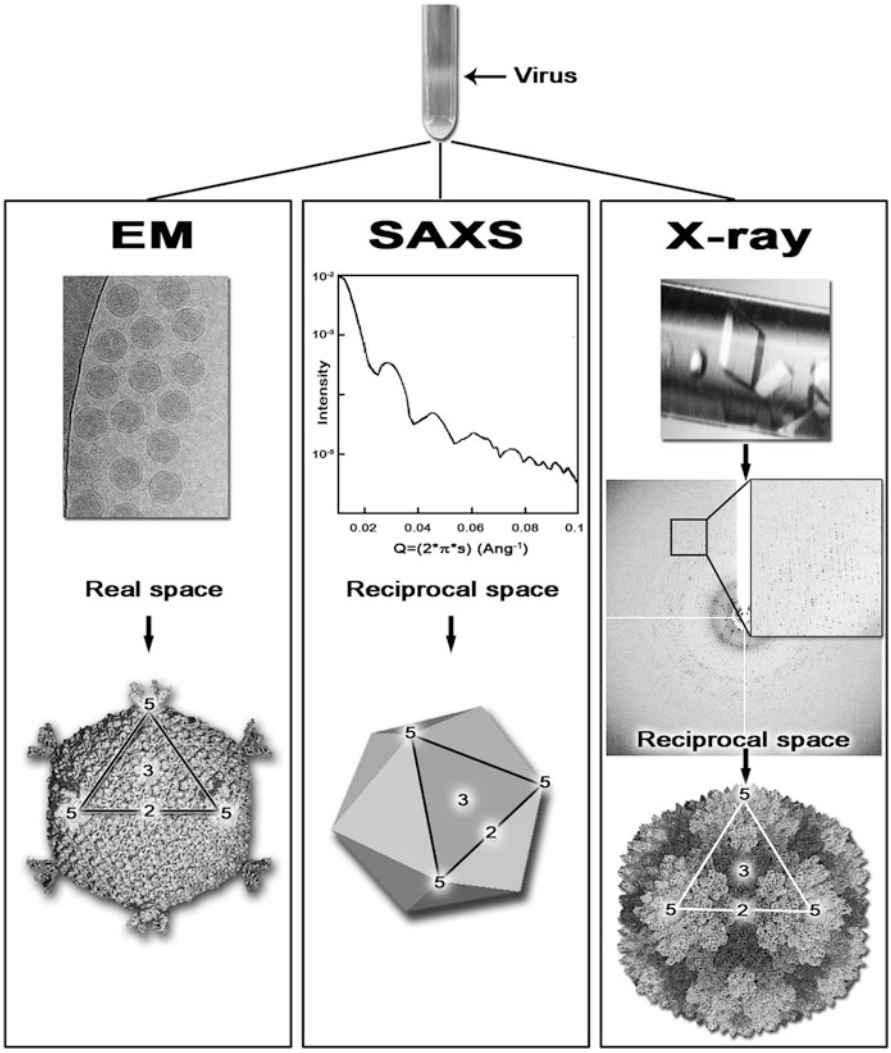

Fig. 7.2 Three major structural techniques at glance. Schematic representation of the workflow of virus structure determination in EM, SAXS and X-ray. All three techniques require purified virus; at the top, a *black arrow* indicates virus band resulting from ultracentrifugation. In EM the purified virus is placed on a microscopy grid, flash-frozen and then the 2D projections of the virus are visualized in an electron microscope producing real space images (*top*); post-processing of these images provides the virus structure (*bottom*). In SAXS the purified virus in solution is irradiated by an X-ray beam producing a low-angle scattering curve (*top*) containing raw data in reciprocal space; post-processing of the data produces the virus overall shape and molecular architecture. In X-ray crystallography the purified virus is used to obtain virus crystals (*top*) that are then diffracted producing diffraction images (*centre*) containing raw data in reciprocal space; once the data processing has been completed and the phase-problem solved, the virus structure is obtained at atomic resolution (*bottom*). The outlined region in the virus models in EM, SAXS and X-ray panels delineates delineates one of the 20 viral facets, and numbers indicate icosahedral symmetry axes (two, 2-fold; three, 3-fold; five, 5-fold). Each technique provides structural information in a different resolution range; in some cases these ranges overlap (see Fig. 7.4)

however in recent years it has become possible to get useful but lower resolution (perhaps 30-Å) data from an individual virus particle by collecting a full tilt series and doing a tomographic reconstruction (electron tomography, ET) (Chap. 3). Furthermore the resolution of both of these methods (EM and ET) can be enhanced for symmetrical virus particles by applying symmetry constraints (see Sect. 7.5.2). X-ray and electron methods begin to almost fully overlap when we consider X-ray microscopy, an emerging technique which is beyond the scope of this review to discuss, but it can simply be seen as a lower resolution, higher contrast version of ET capable of visualising specimens as thick as a eukaryotic cell [6]. Together this armoury of methods allows, for instance, the visualization of viruses and/or replication factories in-situ within the cell (see below and Chap. 14).

7.2.2 *Small-Angle X-ray Scattering*

SAXS is a technique that provides a structural characterization of a protein, protein complex or virus by using the elastic X-ray scattering from a solution containing the system of interest. The mathematical principles of small angle scattering were laid down in 1931 by André Guinier (Fig. 7.1) [for a review see [7]]. As used for the analysis of virus structure it is usual to work in solution phase and to use an X-ray (SAXS, wavelength usually ~1.5-Å) or neutron beam (SANS) onto a homogenous solution containing the biological specimen and to record the one-dimensional plot of scattered beam as a function of scattering angle (Q in the terminology of this method) close to the undeflected beam leaving the sample solution (hence "small-angle"). This one-dimensional scattering profile is the average of all scattering profiles deriving from the individual molecules (Fig. 7.2). Thus, in comparison to EM, where individual slices of the virus particle transform are assembled to produce as complete as possible version of the 3D transform, in small angle scattering the virus particle transform is spherically averaged to produce the linear scattering profile. Despite this massive loss of data, it is possible to extract information that relates to the volume, radius of gyration and the shape of the biological object. Modern synchrotron radiation sources are capable of producing highly acute curves which can support precise interpretation. Due to the development of sophisticated software which uses the massive computational power available today, it is, remarkably, possible to gain *ab-initio* low-resolution structural information by the use of the randomly distributed dummy atom modelling approach that has replaced the original trial-end-error shape assignment [8]. In brief, a large number of differently shaped molecules are generated and the scattering patterns simulated by analytical calculation are correlated and compared with the experimentally measured profile. Additional and/or external knowledge on the sample, for example disulfide-bonds presence, oligomerization state etc., will put constraints on the generation of the different models thereby increasing the reliability of the final shape assigned by the *ab-initio* procedure. Nonetheless, it is not possible to reconstruct a detailed 3D structure of a biological macromolecule from solely SAXS data due to the limited dimensionality of the raw data recorded (Fig. 7.2).

SAXS has been used in the characterization of the shape and composition of viruses since the early days of structural virology. Leonard and co-workers in 1953 carried out SAXS studies on SBMV, TBSV and TNV, in the same year the structure of the DNA was deduced from X-ray diffraction images (Fig. 7.1). At that point no virus structure was solved at high-resolution, but TBSV and TMV had already been crystallized and showed striking diffraction patterns. It is worth mentioning along this line that though not strictly SAXS, wide-angle diffraction and the interpretation of X-ray scattering from a partially ordered specimen, often referred to fibre diffraction have been pivotal in the elucidation not only of the DNA structure but also of virus structures such as TMV or phage Pf1 (for an exhaustive review on fiber diffraction studies of filamentous viruses see [9]). The use of such ordered fibres for structure determination has declined and nowadays is a technique almost unused.

In the early days turnip yellow mosaic virus, cucumber mosaic virus and bromegrass mosaic virus (BMV) were also investigated by SAXS. Interestingly, in the BMV study SAXS data were used alongside negative-stain images of the virus obtained by EM to reveal the virus dimensions and the presence of a hollow structure in the centre of the particles. The small set of plant viruses already mentioned were the initial common targets for the different structural techniques. A deviation from this theme was the structural study of a marine bacteriophage, PM2, the first phage to have been described possessing an internal lipid-bilayer [10]. This painstaking work combined both SAXS and negative-stain EM methods to describe in detail the architectural organization and assembly of proteins and lipids within the phage. Finally, fourty years later the *quasi*-atomic model of the entire PM2 virion was revealed by X-ray crystallography [11]. In retrospect the value of the method is evident – where specific questions can be asked, such as the radius or particle shell thickness and it is possible to construct a unique model, the method can give highly accurate answers and distinguish between competing models. This is exemplified by the results from neutron diffraction.

As with SAXS, SANS has provided insightful information of virus structures exploiting the differential contrast generated by the different interaction of neutrons with the nuclei of water (^1H_2O) and deuterated water (^2H_2O) to spatially map the genome and lipids from the protein mass [7]. Indeed, the advantages of this systematic contrast matching lies in the fact that since the intensity pattern measured (see Fig. 7.2) is the spherically averaged Patterson function defined as the Fourier transform of the structure factors describing the particle embedded in the solvent (for more details on Patterson function see general references on X-ray crystallography provided in Chap. 4), whole sets of Patterson vectors are eliminated by matching out certain components – disturbing markedly the diffraction.

In recent years SAXS has been re-emerging as an important structural tool to study biological macromolecules thanks to synchrotron radiation but also to automation in sample preparation and new high-capabilities of the DECTRIS-Pilatus detectors (see for example some of the European initiatives at http://www.saxier.org/ and at http://www.biostruct-x.eu/). However, from the virus point of view major insights using SAXS should be expected in the study of kinetic and time-resolved processes of virus assembly and disassembly which have started to appear [12].

7.2.3 X-ray Crystallography

In contrast to TEM and SAXS, virus X-ray crystallography (Chap. 4) relies on viruses ordering themselves in a 3D lattice, a crystal (Fig. 7.2). Illuminating the crystal by X-rays then allows one to record the Fourier transform of the unique portion of the lattice (unit cell) and hence the transform of the virus particle. The transform can only be sampled at those points specified by the Bragg condition, however this still allows a fully detailed reconstruction to be produced if all of the unique Bragg spots are measured and phases can be determined (see Chap. 4). Radiation damage is ameliorated since it is spread across all of the particles in the illuminated portion of the X-ray beam – usually in excess of a billion particles. All viruses crystallized so far possess icosahedral symmetry [icosahedron: a platonic solid with 20 identical equilateral triangular faces, 30 edges and 12 vertices; see Chap. 2 for details]. Due to this regular isometric shape, crystallization is often not the bottleneck in a virus crystallographic project and this is particularly true for relatively small and biochemically stable viruses. Indeed, the stability of virus crystals decreases with the increase of the virus size and it is approximately proportional to the inverse of the square of the virus radius [13]. Limitations in the amount or heterogeneity of the purified virus are the most restrictive factors in a successful project. However, recent advances in nano-crystallization techniques and efficient data collection strategies have allowed the determination of virus structures using only approximately 30 μg of virus as in the case of equine rhinitis A virus [14]. Once the crystals are available and show useful X-ray diffraction patterns, data recording and processing, phase determination and refinement with subsequent model building and refinement lead to the final atomic virus structure (for details of the entire protocol see Chap. 4 and [13]).

Thus, X-ray crystallography allows the determination of the virus structure at the atomic level and has contributed and still contributes to a very large extent to the understanding of virus biology. Milestones in structural virology (Fig. 7.1) have been the TBSV structure, the first virus solved at 2.9-Å resolution by Harrison's group in 1978 [1] and the structure of SMBV solved at 2.8-Å resolution by Rossmann's group in 1980 [2]. Five years later the structure of two viruses infecting humans, poliovirus and the common cold virus were solved by X-ray crystallography [15, 16] (see Chap. 4). Since then more virus structures have been elucidated by this technique as witnessed by the number of entries in the Protein Data Bank (PDB). The maximum number of virus structures was deposited in 2000. After this, the rate has decreased. In spite of this trend, in 2004, a significant contribution in the field came from the study of bacteriophage PRD1. PRD1 is the first and the only virus with an internal lipid-bilayer so far solved by X-ray crystallography in atomic detail, revealing a general principle of virus assembly scalable to very large viruses [17, 18].

Finally, in 2010, after several years of parallel advances, both X-ray crystallography and electron microscopy stunningly converged in terms of resolution achieved (~3.5-Å) with the elucidation of the structure of adenovirus (~900-Å diameter), which is so far the largest structure to be successfully tackled by X-ray

crystallography [19, 20]. Meanwhile the methods for the determination of protein structure by X-ray crystallography have become much more routine, in part thanks to efforts to systematise all aspects of the process by structural genomics/proteomics activities [21]. Methodological improvements have also impacted whole virus studies for instance data collection directly from crystallisation plates should make structure determination more routine and safer [22, 23] and continued developments at synchrotrons, including microbeams [24] and pixel array detectors indicate the viability of the method. An area currently unexplored is the use of nanocrystals at highly powerful pulsed X-ray sources (the so-called X-ray free electron lasers). Recent work suggests that structure analysis might be possible from much smaller arrays of viruses than has been possible with more conventional synchrotron sources (see Sect. 7.6.1 and Chap. 4). Different public databases [see *e.g.* PDB http://www.rcsb.org/pdb/home/home.do, http://www.ebi.ac.uk/pdbe/emdb/ and http://viperdb.scripps.edu/] bring together all structural information available on studied viruses.

7.3 Combining X-ray Crystallography and Electron Microscopy

7.3.1 General Approach: The Beginning of Quasi-Atomic Models

Since early times structural virologists have tried to merge information and techniques to provide reliable insights into virus structures. Prior to 1978 (when X-ray virus crystallography first revealed the atomic details of a complete virus [1]), SAXS, EM and X-ray diffraction were usually combined to cross-validate the low resolution information gathered by each individual technique. Increasingly powerful electron microscopes and the definitive establishment of protein and virus X-ray crystallography as a high-resolution technique have made it possible to combine structural information at different resolution levels yielding *quasi*-atomic virus models capable of predicting molecular interactions within the virus or between virus particles and ligands, including virus-host cell recognition processes and virus-antibody interactions.

EM and cryo-EM allow visualization and 3D reconstruction of whole viruses and virus-ligand complexes that cannot be studied by X-ray crystallography. At the same time X-ray crystallography can frequently provide atomic snapshots of the composite pieces of the virus and, as in a 3D jigsaw, structural virologists collate the different pieces to produce the most accurate and precise representation of the virus and its interaction with other (macro)molecules of the outside world. This process defines the procedure of fitting X-ray protein structures, either viral proteins or ligands of the virus into density maps of viruses and virus-ligand complexes obtained by EM and cryo-EM. Despite the fundamental differences in the way electrons and X-rays interact with matter, the end result of 3D analyses in each is a

'density' map which looks surprisingly similar between the two methods and can therefore be interpreted and analysed in a similar way, using similar software. It is important to mention that NMR spectroscopy, although it cannot tackle a whole virus structure, has provided structures of viral proteins that have been subsequently used for fitting into EM maps (see Chap. 5). NMR is also increasing its role as hybrid method providing constraints on possible dynamic events or conformational changes of virus structural components (see Chap. 5).

After an initial manual docking of the entire viral and/or ligand protein structure into the corresponding volume of the EM reconstruction aided by graphic computer programs, improvement and refinement of the fitting carried out in either real space or reciprocal space, can be performed using a correlation coefficient-criterion and/or a least-square minimization [25]. As a result, this rigid-body refinement protocol aims to determine a total of six parameters, a rotation matrix and a translation vector to optimize the fitting to the virus map (Fig. 7.3a). It goes without saying that for a successful fitting the scale of the EM derived density map has to match that of the atomic model.

It has been estimated that this procedure can reach an accuracy of 2.2-Å in a virus map of 22-Å resolution and of 4-Å in a 24-Å map [27], the higher the resolution of the map the better the docking. Programs available for this task include the General Averaging Program (GAP; D.I. Stuart and J.M. Grimes, unpublished software available upon request from authors), EMfit (http://bilbo.bio.purdue.edu/~viruswww/Rossmann_home/softwares/emfit.php), Situs (http://situs.biomachina.org/index.html) and UROX (http://sites.google.com/site/xsiebert/urox). Recently, the concept of flexible fitting has also been introduced that allows distinct domains of the fitted structure to undergo conformational changes to match the volume restrictions imposed by the low-resolution EM map, cf. Norma (http://www.igs.cnrs-mrs.fr/elnemo/NORMA/) or Flex-EM (http://salilab.org/Flex-EM/). One of the critical points in flexible fitting is how to define what is fixed and what is flexible. This can take advantage either of prior knowledge or of normal mode analysis (*e.g.* Norma) that mathematically assigns directions of motion to structural elements of the structure to be fitted. Either approach to the definition of the rigid bodies has its own strengths and weaknesses, for example a user might tend to be over conservative and not reflect the dynamic properties of the structure shown by the EM reconstruction whilst with normal modes the assignment of too many motions can lead to over interpretation.

However, if the resolution of the virus map reaches 7-Å then it becomes possible to identify the fold of the most ordered part of the virus, cf. of major capsid proteins, and to model it using templates for β-barrel or α-helical motifs [28]. It is also possible to adopt template substitution methods, such as those provided by the Rosetta software [29] for modelling into low resolution X-ray and EM derived density maps (4–7 Å).

Nevertheless a major problem when combining different levels of information and specifically in generating (virus) quasi-atomic model is how to finely balance prior knowledge relative to the resolution achieved. In Fig. 7.4 we show the number of effective data points *vs* parameters for the different methods allowing the reader

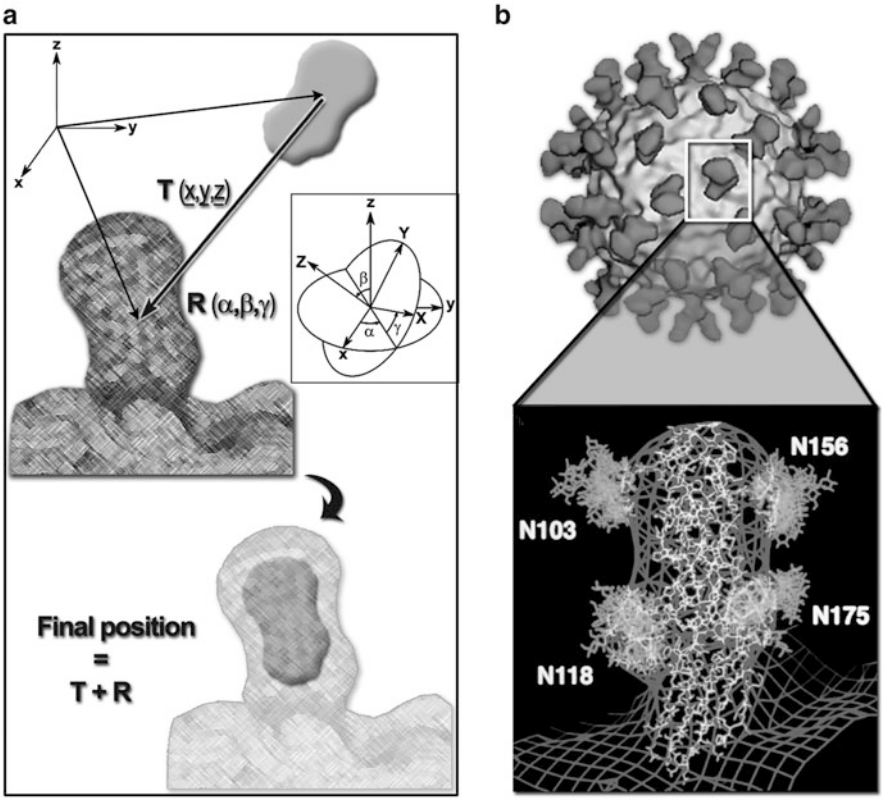

Fig. 7.3 Fitting X-ray data into EM maps. (**a**) Schematic of the fitting procedure; the crystal structure of a virus-binding molecule (ligand, represented here as a *grey* two-lobe object) is moved coarsely from its initial position into the corresponding electron density map of the virus-ligand complex obtained by EM (*dark-grey mesh*) by a translation (*T*) and a rotation (*R*); the final position of the object within the density is achieved by the refinement of six parameters [x, y, z and α, β, γ (Euler angles; inset)] using either real- or reciprocal-space refinement procedures (see [25]). (**b**) *Top*, EM reconstruction of rhinovirus 16 (*light-grey*) with CD155 cellular receptor molecules bound (*dark-grey*); *bottom*, the CD155 X-ray structure (*white* stick model) fitted into the virus-receptor EM density (*dark-grey* mesh); the N-glycosidic groups in the CD155 structure are labelled according to the asparagine residue to which each is bound (Adapted from [26]. With permission)

to grasp what is achievable by each technique and by their combination. In principle we need an objective way of assessing the information content of each of the sources of data and producing a model that satisfies the data to the level of accuracy of the data, but otherwise assumes nothing. We return to discuss this challenge below.

As mentioned earlier, one of the first examples of structural methods combination can be found in the study of adenovirus by Roger Burnett and his laboratory in 1986 [3]. Adenovirus is a large dsDNA virus that infects vertebrates, including

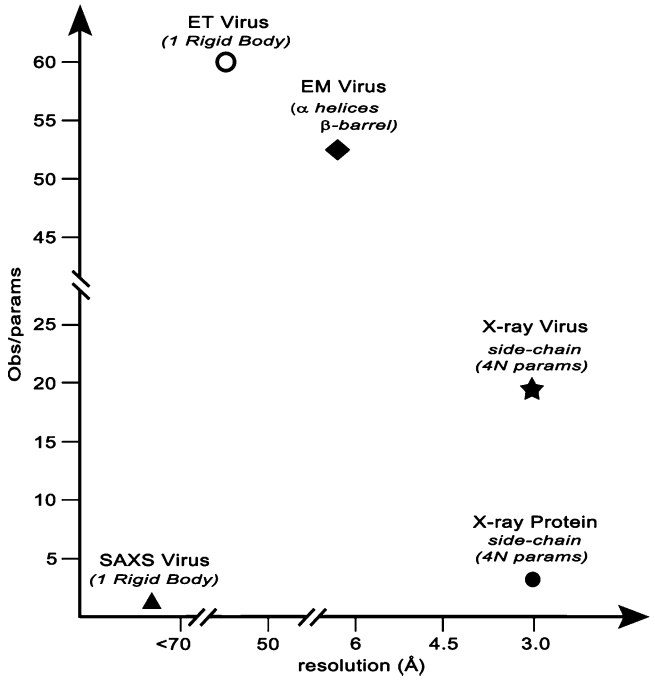

Fig. 7.4 Simplified ratio *per* technique. The data points were obtained by estimating the number of observations for a virus of a determined size and achievable resolution divided the number of structural elements (parameters) to be fitted. For the determination of the virus structure by X-ray crystallography virus we considered the lowest non-crystallographic symmetry scenario in a virus crystal

humans. As passionately stated by Roger Burnett (http://www.cicnetwork.es/secciones/interviews/11_burnett.html) his interest in adenovirus stemmed from beautiful electron microscopy images collected in the '70s by Nick Wrigley of hexamers of the major capsid protein, named hexons that recapitulated architectural elements of the entire virion. However, X-ray structural studies on the hexon structure had already started [30] prefiguring the approach that finally led to the interpretation of protein-protein interactions in the assembling of the large icosahedral adenovirus particle. By solving the X-ray structure of the hexon at 2.9-Å resolution and by placing it into the adenovirus EM reconstruction, Roberts and co-workers [3] opened the way to the hybrid methods approach in structural virology. This has been followed by many other studies for example of the binding of the human cellular receptor ICAM-1 to human rhinovirus 16 (HRV-16) [26], or neutralizing antibody bound to foot-mouth-disease virus (FMDV) [31].

More recently *quasi*-atomic models have been generated for enveloped and membrane-containing viruses. In the former case, a lipid-bilayer decorated by

glycoproteins surrounds a nucleocapsid whilst in the latter case the vesicle is engulfed by the proteinaceous capsid shell. One of the best structurally described enveloped virus is human pathogenic dengue virus (*Flaviviridae* family). Years of investigation on the entire virion by EM and of its glycoproteins by X-ray crystallography have finally produced a clear picture of the dengue virus maturation, assembly pathway and cell-entry mechanism [32, 33]. Also, by combining the crystal structure of an antigen-binding antibody fragment (Fab) in complex with West Nile virus (WNV) E glycoprotein and the dengue and WNV structures in complex with the Fab by EM, Cherrier and co-workers [34] have been able to establish the structural basis for antibody neutralization of infectious immature particles. Likewise *quasi*-atomic models for other biomedical relevant enveloped viruses have been recently generated with a similar 'fitting X-ray structures into cryo-EM maps' approach, for instance chikungunya virus (*Alphavirus* genus, *Togaviridae* family) and vesicular stomatitis virus (*Rhabdoviridae* family).

In the case of lipid-containing viruses, the original example in hybrid methods is PRD1, a bacteriophage that infects gram-negative bacteria [35] and whose *quasi*-atomic model was proposed in 2001 [36]. PRD1 is indeed the model system for this type of viruses having been intensively studied biochemically, genetically and structurally. Its architecture, major capsid protein fold and principle of assembly strikingly recapitulate those elucidated years earlier for adenovirus [3, 17, 18, 37] leading to the concept of viral lineages and virus common ancestry [38] (see below, Sect. 7.8). Another illustrative example, although not strictly a case of fitting X-ray structures into cryo-EM map, is presented by the process that led to the X-ray structure solution of the marine lipid-containing bacteriophage PM2. The moderate 7-Å resolution achieved with the PM2 virus crystals (in comparison to the ~4-Å resolution obtained for PRD1 virus) prompted the determination of the structures of the individual components at higher resolution [11]. This "divide et impera" approach led to high resolution structures of the two major viral capsid components that were then docked into the low-resolution X-ray map. As a result, key aspects of viral evolution, capsid assembly and membrane morphogenesis were elucidated [11].

Furthermore, it is worth underlining that the protocol of fitting of atomic structures into electron density maps can be also extended to volumes obtained by sub-tomogram averaging (see below and Chap. 3; sub-tomogram averaging algorithms [39–41] allow averaging equivalent structures thus improving the signal-to-noise ratio). This can lead to plausible fitting of X-ray crystal structures as in the case of the capsid protein domain of the Gag polyprotein in HIV [42].

Finally, the combination of methods in structural virology has pioneered an equivalent approach nowadays emerging in biology and defined as 'integrative modelling'. Indeed, this approach aims to combine different available sources of information – structural, biochemical, biophysical and proteomics – to obtain a molecular picture or a unified structural view of the system in study. Nice examples of this are embodied in the 'Integrative Modelling Platform' (IMP) (http://salilab.org/imp/) and Haddock (http://www.nmr.chem.uu.nl/haddock2.1/), with a recent example being the analysis of the nuclear pore [43]. How and with what weights the different sources of information are combined remain to be fully and routinely

implemented in a suitable statistical framework (Bayesian, Maximum-Likelihood, etc.) that would provide a validation and statistical significance assessment of the resultant model. Although this work is ongoing and is still very crude in many cases, the vision is already set, thanks to the combination of methods used to study virus structures.

7.3.2 *Validating the Quasi-Atomic Models*

Validation of the proposed *quasi*-atomic model is fundamental to the reliable interpretation of molecular interactions and their usefulness. Although several programs (see Sect. 7.3.1) that carry out positional refinement of the initial docked structure into low resolution maps provide correlation coefficients (for real space analysis), or metrics equivalent to the crystallographic R-factor [44] (for reciprocal space analysis), the inclusion of such values in the final publications is still left to the discretion of the authors. It must be said however that there is no unique criteria that describes the accuracy of the model and a multi-parameter assessment (atomic clashes, stereochemistry, biological meaningfulness) together with the statistical measures is the best solution at present. Furthermore, if additional biochemical or biophysical information is available, for instance a proved interaction between specific residues of the ligand and the virus, then it should be taken into account for example by imposing restraints on the movements of the fitted X-ray structure during refinement.

In 2010, the EM community attempted to standardize practices during the inaugural meeting of the Electron Microscopy Validation Task Force (http://vtf.emdatabank.org/). A series of guidelines and recommendations were suggested with the ultimate goal of increasing the impact and the significance of EM in biology and biomedicine. This reflected the earlier successful efforts of the X-ray community through the X-ray Validation Task Force (http://www.wwpdb.org/workshop/2011/index.html), where the broad principles are now accepted and required for publication. Given the limitations on the validation criteria it is advisable when combining X-ray with EM, to keep a conservative attitude in the biological interpretation of the resulting *quasi*-atomic model. Also, remember that the data-to-parameter ratio generally available during this hybridization process is unfavourable (see Fig. 7.4) – better safe than sorry!

7.3.3 *Phase Information "Interplay"*

A major problem in crystallography, as previously stated, is the so-called phase problem, a methodological 'inconvenience' that prevents the retrieval of atomic

positions directly from the raw data (see Chap. 4). EM images embody the phases of the object, by visualizing it in real space and thus are a potential source of phase information for diffraction methods. When highly symmetrical particles such as icosahedral viruses are investigated structurally, it is possible to exploit the redundancy of information for phase refinement (see Chaps. 3 and 4). In crystallography, in the best-case scenario when none of the symmetry axes of the virus align with the crystallographic symmetry axes of the crystal, the full 60-fold non-crystallographic symmetry (NCS) can be iteratively used to improve the starting phase assignment [in the worst-case scenario only 5-fold NCS]. It has been shown that the availability of 60-fold NCS can allow convergence of phase refinement starting from phases derived from a spherical object [45, 46] (for an overview on *ab-initio* phasing see [47]). However, for this protocol to succeed it is paramount to know (*i*) the exact location of the icosahedral symmetry axis relative to the asymmetric unit (AU) of the unit cell, (*ii*) the radius of the starting model [45, 46] and (*iii*) the protein region for the generation of appropriate envelopes used in the averaging and solvent flattening procedures.

In virus crystallography, apart from the first virus structures that were solved using heavy atom methods [1, 2], it has been and still is a common practice to use as a starting phasing model a virus previously solved [unrelated or even a sphere (see above)] or, if available, a low-resolution derived EM map located within the asymmetric unit of the unit cell of the crystal through the molecular replacement (MR) technique [13, 48] (see Chap. 4). It is worth noting that for the phasing of FMDV [49], a hybrid virus model was built from existing viruses weighting-up the conserved structural pieces and used as a searching model in MR, an approach that is now implemented in some of the standard protein MR protocols.

Advances in EM (see Chap. 3) have propelled the application of this phasing strategy to X-ray data obtained from crystals of biological macromolecules smaller than viruses and often less symmetrical [50–53]. Although there are exciting perspectives of this alternative approach for circumventing the crystallographic phase problem, further requirements need to be fulfilled for its successful application: resolution range overlap between the 3D electron microscopy data and those obtained by X-ray crystallography, *i.e.* it is important to collect the low-resolution terms, and the presence of non-crystallographic symmetry. The former condition allows the object to be located within the asymmetric unit of the unit cell (by MR), while the latter boosts the phase refinement and phase extension procedures. To be more precise the power of phase extension depends on the degree of oversampling of the transform of the unique portion of the object and non-crystallographic symmetry delivers this directly, however a very high solvent content does so as well (for instance a thin virus shell with disordered interior).

One of the first examples in which the use of low-resolution models was successful in phasing X-ray data of a small protein (38 kDa) was inspired by studies on Mengo and FMDV viruses [50]. Villeret and co-workers were not only able to build the correct geometry of the oligomeric state (12-fold) using a monomeric X-ray structure of a related protein and generate low-resolution phases at 8-Å but they were also able to phase-extend those initial phases to the full 3-Å resolution of the X-ray data (see also ‘Further reading’).

In principle also SAXS could provide initial low-resolution phasing as it has been described in the case study of nitrite reductase, a 34.4 kDa protein that forms homotrimers. However, in this case once the SAXS envelope was correctly located in the asymmetric unit of the unit cell, only phases to 20-Å were reliable and no further phase extension was attempted [54].

A recent enlightening case of phase interplay between EM and X-ray crystallography comes from the structure of the marine bacteriophage PM2 at 7-Å resolution [11] (Fig. 7.5). The initial phases for solving the entire virus X-ray crystal were derived from the cryo-EM based PM2 structure at 8.4-Å resolution [55]. In spite of the apparently minimal ~1.4-Å improvement in resolution of the X-ray over the EM data, the quality of the resulting X-ray map thanks to the accuracy of the crystallographically measured structure factor amplitudes, allowed a clearer interpretation of the different, 60-fold symmetrical arranged structural components, in particular those pivotal elements located between the capsid and the lipid vesicle [11]. However, the 7-Å X-ray map could not provide the unequivocal determination of the fold of the major capsid protein P2 (32 kDa). So, an X-ray crystallography study of isolated P2 was undertaken [57]. The failure of MR using supposedly related X-ray structures as searching models, and the difficulty of getting heavy-atom soaked crystals or suitable selenomethionine (SeMet)-derivatized X-ray data (see Sect. 7.4) required the use of the low-resolution electron density corresponding to a P2-trimer extracted from the X-ray averaged map of PM2 as searching model. The location of the two P2-trimers within the asymmetric unit of the cell by molecular replacement led to the determination of the initial phases at 7.6-Å resolution then extended to 2.5-Å by means of non-crystallographic symmetry and solvent flattening [56].

In conclusion, although the examples mentioned above do not yet represent routine procedures, the experience gained in virus phasing provides an additional structure determination tool for protein crystallography.

7.4 Dissecting Virus Structures by Combining Biochemical, Genetic and Biophysical Tools

Virus structures can be tackled by complementing not only the structural techniques mentioned above but also methods that involve the biochemical and genetic manipulation of the virion. It is clear that the prerequisite for high-quality structural data is the quality of the original biological material. The traditional ways to purify viruses are based on their sedimentation behaviours (rate zonal centrifugation) or their particle densities (equilibrium centrifugation). These can then be combined with differential centrifugation, concentration methods (*e.g.* filter devices) or precipitation (*e.g.* using different polyethylene glycols). The addition of biochemical and genetic modifications makes it possible to produce and to study different kinds of virus material from wild type and mutant virus infections, perform quantitative virus particle dissociations experiments, or use recombinant protein expression

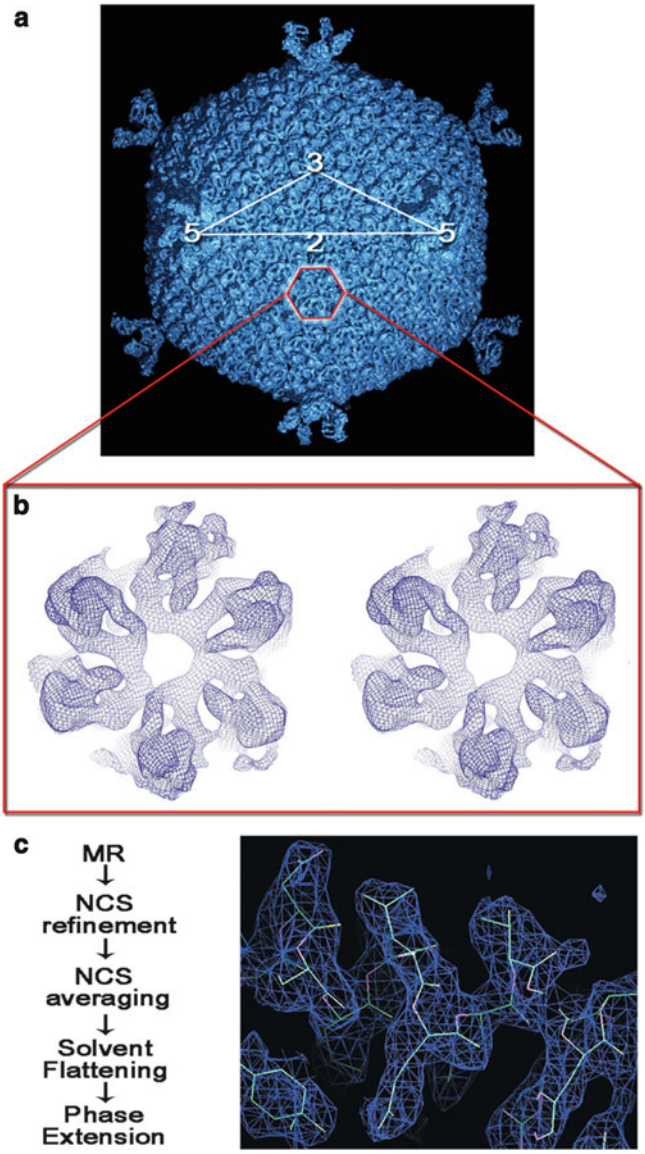

Fig. 7.5 Phasing with low-resolution phases. (**a**) X-ray-derived map of the lipid-containing bacteriophage PM2 [11] (~600-Å in diameter), which was phased using the corresponding EM map [55]; icosahedral symmetry axes in the capsid are labelled; a trimeric capsomer of the major capsid protein P2 is outlined in *red*. (**b**) Enlarged stereo-view of the extracted electron density at 7-Å corresponding to the P2 trimer used in the MR protocol. (**c**) *Left*, workflow for phasing X-ray data using the low-resolution density map in (**b**) as a searching model; *right*, experimental electron density map at 2.5-Å for the P2 major capsid protein resulting from MR, followed by phase refinement, extension and solvent flattening (Reproduced from [56]. With permission)

systems. In the following sections we will illustrate some examples where the tailored use of biochemical, genetic and biophysical techniques has provided insightful views into virus structure.

7.4.1 Classical Antibody Labeling Methods

Immuno-EM can be used as a powerful tool to localize specific proteins also asymmetrically distributed in the virion. The method relies on the specific recognition, by primary antibody, of a target protein (antigen) exposed on the virion surface. A secondary molecule recognizing the primary antibody is then added, for instance, gold-conjugated protein A, which binds with high affinity to rabbit-IgG molecules. The gold particles produce high contrast under TEM (see Sect. 7.2.1) allowing the localization of specific proteins in the virus structure, but detailed structural information is lost. Using secondary binders conjugated to gold particles of different sizes, different antigens can be co-localized within the same sample. Prior to the labelling, the virus particles are usually fixed with cross linkers, glutaraldehyde being one of the most popular choices. Recently the toolbox of cross-linkers and chemical probing protocols available has been expanded [58] allowing the exploration of novel avenues in virus biochemical manipulation. Furthermore, virus particles can be loosened *e.g.* by mild treatment with non-ionic detergent such as Triton X-100 during the sample-grid preparation to increase the accessibility of the antigens to the primary antibodies; see for example [59].

Typical problems of immune-EM, such as unspecific labeling or background can be overcome by having appropriate controls and adjusting the amount of primary antibody. The most reliable conclusions, however, can be made when immunogold labeling EM data is combined with other approaches, as demonstrated for the dsDNA bacteriophage PRD1. Combination of immunolabeling [59] with the work done with PRD1 mutants [60] verified the presence of the unique vertex structure used for genome packaging.

7.4.2 Mutagenesis Studies

Classical mutagenesis using shotgun mutagens such as ultraviolet light (UV) or N-methyl-N-nitro-N- nitrosoguanidine (NTG) and, especially, site-directed mutagenesis are powerful techniques to create virus mutants. To identify proteins and investigate their functions specific virus mutants can be created either by generating a stop codon inside the target gene (nonsense mutants) or by deleting the entire protein coding region (deletion mutants). If the mutations are lethal, rescue systems are needed in a form of suppression or complementation, which limit the usage of virus mutants to those viruses infecting a host for which a genetic system has been

established. Genetic engineering of obscure micro-organisms isolated from the environment is demanding [61]. Bacteriophage PRD1 infects gram–negative bacteria such as *Escherichia coli* and *Salmonella enterica* enabling the use of well-established genetic tools. PRD1 is one example for which numerous suppressor-sensitive mutants have been obtained and have proved invaluable in assigning functions to the corresponding viral proteins. Furthermore, the genetic removal of the PRD1 flexible receptor-binding proteins from the virion vertices was crucial in obtaining diffracting crystals leading to the determination of the X-ray virus structure at 4-Å resolution [17, 18].

Moreover mutagenesis has also allowed the insertion of green-fluorescence protein (GFP) into large and complex viruses such as herpes or vaccinia viruses – providing an important tool for studying cell interactions or virus localization within the cell (see Chap. 14). We expect that careful selection of multiple tags will also provide structural information, *e.g.* from fluorescence resonance energy transfer (FRET) and correlation spectroscopy methods. An early example comes from work on influenza virus polymerase revealing interactions in the cell [62].

Fine structure-function relationships in virus particles at the amino acid residue level can be carried out by individually replacing specific residues based on high-resolution structural information. Classically residues are replaced by alanine, removing the side chain (beyond the Cβ atom) and the intra- or intermolecular interactions it establishes with other residues, without introducing additional groups and non-native interactions, and with the minimum probability of altering the main-chain conformation of the viral proteins. For example, systematic alanine-scanning mutational analyses on the structural and functional relevance of protein-protein and protein-nucleic acid interactions in a virus particle have been carried out for FMDV and the parvovirus minute virus of mice (see Chaps. 1 and 7). Also, resolution of the crystal structure of some designed single-amino acid mutants is providing high-resolution insights into the structural bases of physical properties, assembly, conformational dynamics, and disassembly of virus particles, for example in rhinovirus and poliovirus.

7.4.3 Quantitative Dissociation Studies

The controlled removal of specific proteins from virus particles is very valuable for structural and structure-function studies (Fig. 7.6a). Using this biochemical quantitative dissociation approach several viral proteins have been assigned to their right positions in the virion. The interactions between the capsid proteins and the underlying membrane component can be disrupted by *e.g.* urea or guanidine hydrochloride treatments, as exemplified by studies on bacteriophages PM2 and PRD1, respectively, which revealed the virus membrane associated proteins and released the major capsid proteins [64, 65]. The released proteins can be further purified by standard biochemical methods for protein crystallography [37, 57, 65]. Quantitative protease treatments of the virus particles might identify structures

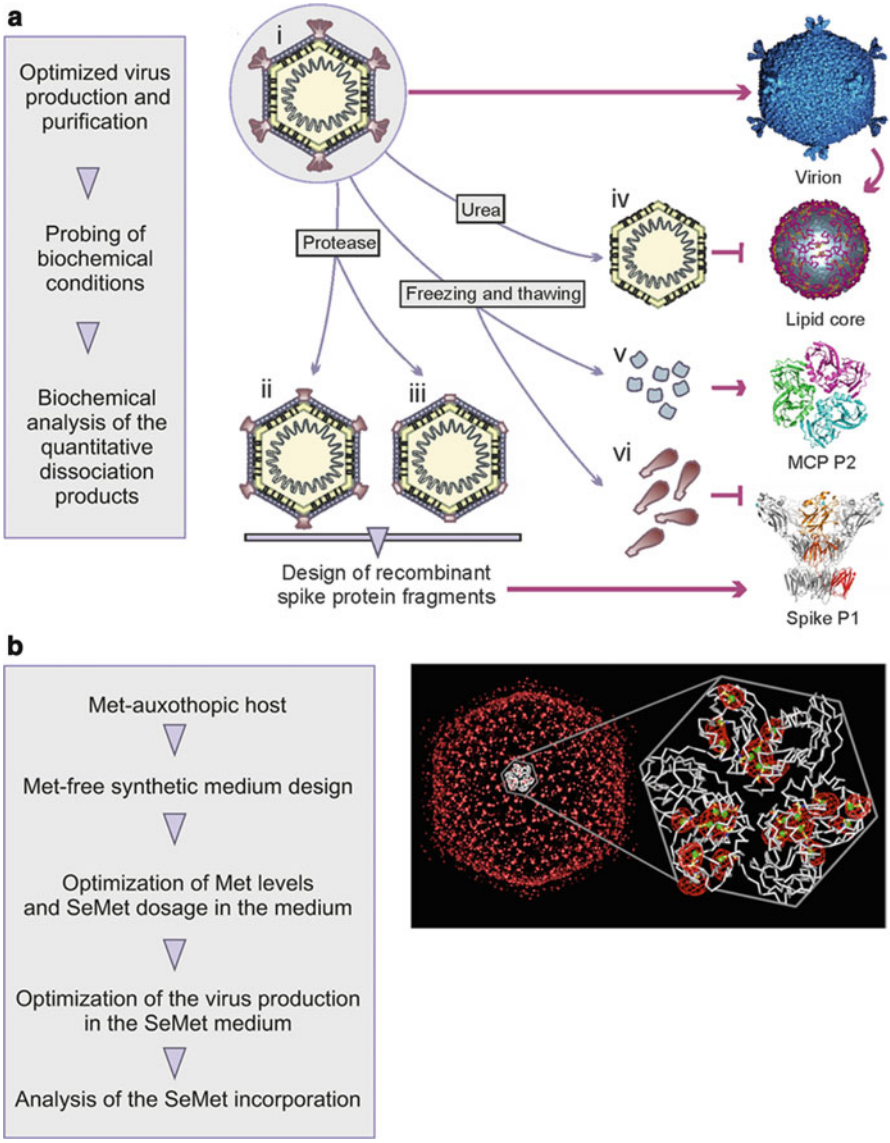

Fig. 7.6 Schematic workflow for biochemical probing. (**a**) *Left*, workflow in a study on the quantitative dissociation of virus particles. *Right*, schematic representation of the controlled dissociation of bacteriophage PM2 [63] used to solve the structures of virion components. (i) Highly purified and infectious virions used to solve the virion structure by cryo-EM [55] and X-ray crystallography [11]; (ii) proteinase K-treated virus particles devoid of the distal receptor binding domain of the spike protein P1; (iii) bromelain-treated virus particles devoid of the two outermost domains of the spike protein P1; (iv) urea treatment expose the internal lipid core particle (membrane proteins, lipids and the genome); (v) and (vi) freezing and thawing of the virions release (v) the trimeric major capsid protein (MCP), and (vi) the monomeric spike proteins.

protruding from the virion surface [55, 65]. For the analysis of membrane-containing viruses, membrane extraction with different detergent treatments can be used to selectively remove different membrane-associated proteins from the virus particle. In case of the internal-membrane containing PRD1 virus integral and peripheral membrane proteins have been separated from one another [66].

One example of a quantitative dissociation analysis is marine icosahedral dsDNA bacteriophage PM2 (Fig. 7.6b). For PM2, several unique subviral particles have been distinguished by their sedimentation properties in a sucrose gradient [55, 65]. A combination of biochemical, cryo-electron microscopic [55] and X-ray crystallographic approaches [11, 56, 57] has visualized the entire PM2 virion structure at subnanometric resolution and led to the determination of its major structural protein structures (Fig. 7.6b). Also archaeal virus SH1 [67], archaeal pleomorphic viruses [68] and *Thermus* bacteriophage P23-77 are examples of viruses for which quantitative dissociation analysis has provided useful information and significantly helped in the structural analysis [69].

7.4.4 Selenomethionine Incorporation as a Labelling Tool

Efficient selenomethionine labelling of protein species within bacteria is nowadays a standard technique but less so for the labelling of proteins expressed in mammalian cells [70]. Even more challenging is the selenomethionine labelling within viruses that when combined with X-ray crystallography is a valuable method in the structural virology. To date, only two efficient methods for selenomethione labeling of complex viruses have been reported [63, 71] and their roles in the interpretation of the electron density maps of PRD1 and PM2 were significant [11, 17, 63]. The PM2 labeling method relied on methionine auxotrophic host (Figs. 7.6c and d; [63]), whereas successful PRD1 selenemothionine incorporation was obtained with methionine prototrophic host grown in minimal medium and pulsed with selenomethione at a late stage of infection [71]. In addition to obtaining phase information in X-ray crystallography [72], selenomethionine labeling combined with difference Fourier maps can facilitate the interpretation of protein folds and even the identification of the protein species [11]. Using selenomethionated and native virus X-ray data it was possible to assign electron density to all ordered protein components in the virion based on their amino acid sequence [11, 63].

Fig. 7.6 (continued) *Far right, top to bottom*: X-ray crystallographic structure of a virion and its lipid core particle, MCP P2 trimer and the pentameric vertex-spike complex of protein P1 (Adapted from [11]. With permission) (**b**) *Left*, workflow of the selenomethionine (SeMet) labeling of bacteriophage PM2. *Right*, SeMet difference Fourier map for the entire SeMet-labeled PM2 virion contoured at 4σ (*red* mesh) with a single trimer of the MCP P2 outlined in *white*; an enlarged view of the P2 Cα backbone is shown, with the methionine residues depicted as balls-and-sticks (the incorporated selenium atoms are shown as *green spheres*) (Reproduced from [63]. With permission)

7.4.5 Some Old and New Biophysical Techniques to Study Viruses

Together with the above techniques other biophysical methods for studying virus particles in solution, including fluorescence spectroscopy, circular dichroism (CD), hydrogen exchange or limited proteolysis followed by MS (see Chap. 6) and differential scanning calorimetry (DSC) and isothermal scanning calorimetry (ITC) may be used to study different aspects of virus particle stability and conformational dynamics, and relate these properties to virus structure. DSC and ITC respectively are useful in assessing the thermal stability and conformational transitions of virus particles and in the study of virus/cell binding, entry processes and genome release. Several studies have been carried out using DSC and ITC on viruses and phages, cf. phage λ [73]. Changes in secondary structure of the capsid proteins in viral particles have been followed by far-UV CD; intrinsic fluorescence of viral particles or extrinsic fluorescence by binding dyes to the viral nucleic acid exposed on capsid disassembly have been used to follow capsid conformational rearrangements and determine the thermal or chemical stability of viral particles against dissociation (see Chap. 6).

Recently an application of the thermofluor assay used to assess protein stability before crystallization has been adapted for high-throughput screening of thermal stability of viruses [74]. This new application uses two distinct fluorescent dyes simultaneously, one with affinity to hydrophobic residues and the other to the genome. Upon heating, hydrophobic residues becoming exposed and genome release are simultaneously monitored by the fluorescence intensity and virus stability rapidly assessed.

Finally, recent developments in MS techniques have shown that it is possible to investigate very large protein complexes such as viruses by native MS (see Chap. 6). This formidable advance [75] opens the way to the analysis of virus disassembly processes traditionally considered out-of-range for this method.

7.5 Combining Electron Microscopy and Electron Tomography

7.5.1 General Approach

The understanding of the architectural and molecular organization of enveloped and complex viruses is a current challenge. Traditional approaches such as EM and more stringently X-ray crystallography require sample homogeneity in terms of structural organization and size, a premise that fails when studying those viruses that do not possess a regular shape or composition, the so-called pleomorphic viruses. Indeed such viruses often come in several sizes and shapes and the lack, until recent years, of a structural technique that could tackle such viruses had left them at the margin of structural investigation.

The advent of ET and cryo-ET [76] (Chap. 3) has allowed these difficult viruses to be tackled [77]. With this technique (for details and some examples see Chap. 3) viruses can be studied as individual particles whilst those structural elements conserved and redundant within the virus structure can be averaged, thus improving the signal-to-noise ratio and overcoming typical problems inherent to the technique such as anisotropy and incompleteness of data due to the missing wedge [76].

Thus, if a virus possesses distinct structural levels some with no symmetry (*e.g.* envelope) and others with symmetry (*e.g.* nucleocapsid) it is in principle possible to combine the cryo-ET 3D reconstruction with the other symmetry-imposed and/or averaged structural elements. These latter elements are usually at higher resolution and can be either obtained by sub-tomogram averaging within the same tomographic data collection (see for example [39, 41] and websites http://www.dynamo-em.org; http://www.biochem.mpg.de/en/rg/foerster/Content_Software/PyTom/index.html; http://www.opic.ox.ac.uk/mediawiki/index.php/Jsubtomo) or by other structural methods such as EM or X-ray crystallography. This combination will picture the architectural complexity of the virus at different resolution levels. ET is also very powerful in studying viruses in the cellular context, in particular during viral entry and replication (see also Chaps. 3 and 14). In the following section we will give a few examples of the combination of ET and EM techniques and we will illustrate the smart use of tomography in assessing particle symmetry [78].

7.5.2 Case Studies

One of the most elegant examples of combination of EM techniques in picturing a complex virus is the cryo-ET study of herpes simplex virus (HSV) [79]. In this work the regular icosahedral nucleocapsid was separated from the enclosing pleomorphic envelope in turn decorated by the tegument and glycoproteins, both indispensable for infection. Nucleocapsids were extracted from the tomograms, 60-fold averaged (as in standard icosahedral 3D reconstruction approach) and replaced in the whole virus 3D reconstructed tomogram (Fig. 7.7a), thus revealing contacts between the nucleocapsid and the tegument not seen in individual tomographic reconstructions.

Combination of ET and EM is not limited to viruses with an intrinsic symmetry mismatch. Several situations during the infection cycle induce a symmetry loss even in highly symmetric viruses. Picornaviruses are small, icosahedral, non-enveloped viruses that have been studied for several viral processes such as receptor attachment or RNA translocation. The use of decorated liposomes with poliovirus receptor CD155 allowed the imaging of the receptor bound to poliovirus both by single-particle reconstruction and electron cryo-tomography [82].

For retroviruses, cryo-ET has provided structural information of the human and simian immunodeficiency viruses (HIV/SIV) envelope spike proteins gp41/gp120 (Env) responsible for binding to the cellular receptor. The gp120/gp41 complex is randomly distributed onto the virion surface making it difficult to study [83, 84].

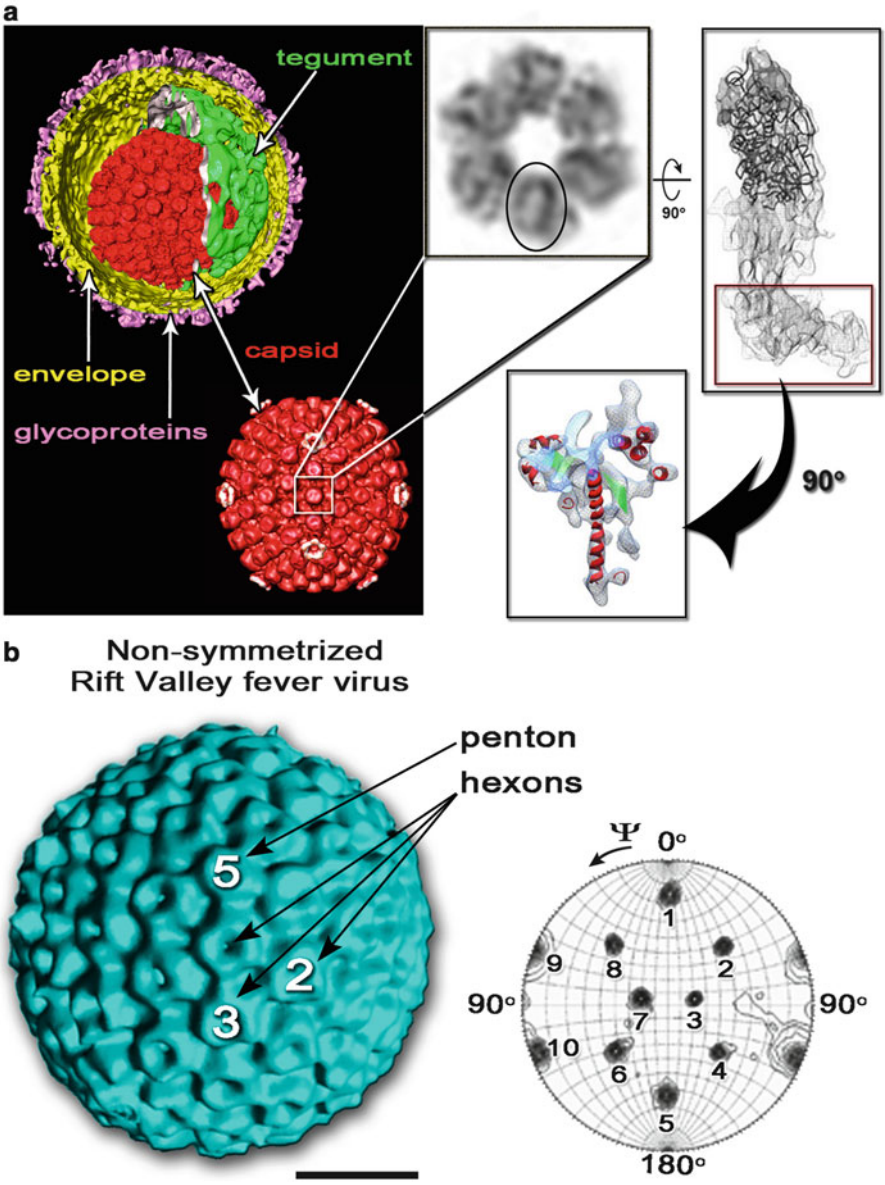

Fig. 7.7 Using X-ray tools in electron tomography. (**a**) *Top left*, herpes virus electron cryo-tomography reconstruction with the different structural elements [79]; below, herpes virus nucleocapsid reconstruction obtained by sub-tomogram averaging combined with icosahedral averaging; outlined one capsomer sitting on a 2-fold icosahedral axis (Courtesy of K. Grünewald, University of Oxford); *top center* cryo-EM derived density corresponding to this capsomer which is composed by six copies of VP5 protein; *top right*, a VP5 monomer composed of three domains (upper, middle and floor domain); the crystal structure of the upper domain is shown as a Cα ribbon model (*dark-grey*) fitted into the corresponding cryo-EM density; no X-ray structure exists for the

Subtomogram averaging of thousands of individual spikes and the imposition of the threefold symmetry gave a 3D map of sufficient quality to dock in the structure of SIV-gp120 core previously solved by X-ray crystallography [85]. Additional studies with bound receptor and antibody have elucidated key aspects of the spatial arrangement during cell and antibody recognition and conformational tuning [86]. Moreover beneath the HIV/SIV envelope, during maturation and after cleavage of the Gag polyprotein, the capsid domain forms the cone-shaped core shell organized as a hexagonal lattice. Tomographic images of this lattice followed by subtomogram averaging of the hexagonal building block allowed individual protein domains to be identified and fitted with the corresponding X-ray crystal structure [42].

Cryo-ET has also provided a 3D picture of influenza virus that displays an evident pleomorphy [87]. The two different surface proteins could be distinguished directly from the tomograms and molecular shape comparison with the crystal structures of hemagglutinin (HA) or neuraminidase (NA) allowed mapping of the individual spikes in the tomograms.

Preliminary analysis of negatively-stained samples of several bunyaviruses showed a large diversity in size, morphogenesis, structure and surface. One member of this virus family is Rift Valley fever virus (RVFV), a major pathogen of animals and humans in Africa. Cryo-ET provided the first useful 3D reconstruction of the RVFV [78], achieved by reconstructing 46 individual particles with similar overall size and shape and then averaging them together. The averaged map was Fourier transformed and the derived structure factor amplitudes used to calculate a self-rotation function [a routine procedure used in X-ray crystallography to detect the redundant presence of structural elements within the asymmetric unit of the crystal (see Chap. 4), Fig. 7.7b]. This identified five-, three- and twofold axis and allowed the unambiguous assignment of icosahedral symmetry to this virus. In turn, imposition of the 60-fold icosahedral symmetry further improved the resolution of the 3D reconstruction from 75-Å to 61-Å, revealing the capsomers arrangement and the symmetry of the lattice (triangulation number *pseudo*-T = 12). This laid the basis for structural studies at higher resolution that was achieved by the systematic single-particle sub-tomogram averaging of 267 particles, leading to a virus map at 20-Å resolution. This dramatic improvement allowed the analysis of the structure of the heterodimer formed by the G_N and G_C glycoproteins which decorate the envelope [88].

Fig. 7.7 (continued) middle domain; the floor domain is delineated by a *red rectangle* (Figure adapted from [80]. With permission). *Bottom right*, cryo-EM density corresponding to the floor domain; secondary structure templates have been fitted to suggest structural homology with the gp5 capsid protein of bacteriophage HK97 (Figure adapted from [81]. With permission). (**b**) *Left*, electron density reconstruction of RVFV by single particle electron tomography [78]; capsomers and icosahedral 2-, 3- and 5-fold symmetry axes are marked; *right*, stereographic projection of the Kappa = 120° section for the self-rotation function of the tomographic reconstruction, revealing the presence of 10 3-fold axes, and thus demonstrating the icosahedral nature of the RVFV; scale bar represents 25 nm (original images courtesy of SJ Watowich, University of Texas Medical Branch)

7.6 From Viruses in Solution to Virus in Cells

7.6.1 Virus Structures in the Cellular Context

Viruses have been traditionally observed within infected cells using either fluorescent labelled viruses and light-microscopy (resolution worse than 200-nm) or using cell-sectioning techniques for subsequent imaging in an electron microscope [4] (see Chap. 14). In this latter case different cell and sample preparation techniques have been put in place and optimized to preserve close-to-native conditions of the virus and cell. These efforts have been coupled to advances that have made the acquisition of tomographic data routine. Tomography thus allows adding depth information at higher resolution than the serial addition of ultrathin 2D sections (for details and examples see Chaps. 3 and 14).

One of the most recent additions to the available tools to investigate virus structures has been provided by synchrotron facilities through the generation of soft X-rays in the water window (wavelength 2.3–4.4 nm) that due the differential absorption of oxygen and carbon atoms (ten times lower for O than C) provide contrast for cellular tomography imaging. Virus X-ray tomography has seen pioneering applications using as model systems the virus life cycle of vaccinia virus [89] and herpesvirus [6]. These studies demonstrate that soft X-rays can provide valuable 3D structural insights into virus maturation events at the sub-nanometer level (50–30 nm resolution) for reasonably thick (5–8 μm) cells and compartments, including the cell nucleus.

Interestingly, virus crystallography is also aiming towards *in vitro* structural analysis. Indeed crystals of large viruses are extremely fragile and there are attempts to grow intracellular crystals for structure determination – a grand challenge for crystallography (see also Chap. 4). Inspirational of this new crystallogenesis strategy has been the observation that not only does protein crystallization occur *in vivo* [90, 91] but also paracrystalline arrays of virus particles often form within infected cells [4, 92]. However further developments in synchrotron radiation technology in particular in delivering high-brilliance synchrotron light, are needed to make X-ray data collection possible from these *in vivo* crystals and hopes are raised by the preliminary tests of the X-ray free electron laser (XFEL) on viruses [93, 94], that although technically successful provided very low resolution information (<200-Å) due to the limited number of incident photons in each short pulse of X-rays.

7.6.2 Methods for Cellular Landscape Scanning

One of the major difficulties in the structural interpretation of virus-infected cells is the confusion deriving from macromolecular crowding. In order to be able to provide an atlas of the different steps of a viral infection, following how the viruses enter the cell, replicate and assemble, and finally leave the cell, different timeline

points are structurally investigated during infection (see Sect. 7.7.1). For each timepoint tomograms are collected and combined computational techniques, from segmentation to template matching, are employed to detect recurrent cellular or virus structures [95, 96]. Sub-tomogram averaging of equivalent structures increases the signal-to-noise ratio and allows the improved structure to be inserted back into the cellular landscape [97, 98]. This approach can also use virus structures obtained at higher resolution by other methods such as cryo-EM or X-ray crystallography, thus providing more accurate information about the geometrical arrangement and spacing between virus particles and cellular structures. This hybrid approach fills-in information inevitably missing from grid-based ET methods (see Chaps. 3 and 14) and bridges the resolution gap between 3D cellular tomography and other methods such as single particle EM and X-ray crystallography [92].

7.7 Emerging Hybrid Methods

7.7.1 Correlative Microscopy

The analysis of biological functions from whole organisms to cells and subsequently to single molecules has been a dream for structural scientists for decades. Structural biology and virology has recently become increasingly interested in dynamic cellular and virus-cell interaction processes This requires a time-resolved approach to the visualization at the different size levels and the correlation in time and space between the different methods remains a challenge.

Correlative microscopy allows the integration of data across the microns to nanometers range, using fluorescence light microscopy and electron microscopy [6, 99, 100] (see Chap. 14). However, from the point of view of combined structural strategies it is important to underline that the aim is to identify cellular regions of interests by the use of specific chromophore labels in the light microscope and track biological events before stopping the clock and imaging the same region at much higher-resolution using an electron microscope. In this way virus-cell interactions are reconstructed in 3D and framed in time. A critical step is finding the same cellular region once the cell is within the electron microscope. To this end a common reference system between the light- and electron-microscopes must exist. Technological advances in robotics and microscopy cryo-holders have made possible data collection and a general work-flow for the procedure, pioneered by Plitzko [99] (Fig. 7.8). While correlative microscopy for 3D tomographic reconstruction is still in its infancy the potential benefits are enormous in studying virus-infected cells. Recent important contributions come, for example from the study of retroviruses where it has been possible to identify HIV particles attached to cell membranes [101] and to show the release of mutant HIV cores into the cytoplasm of host cells [102].

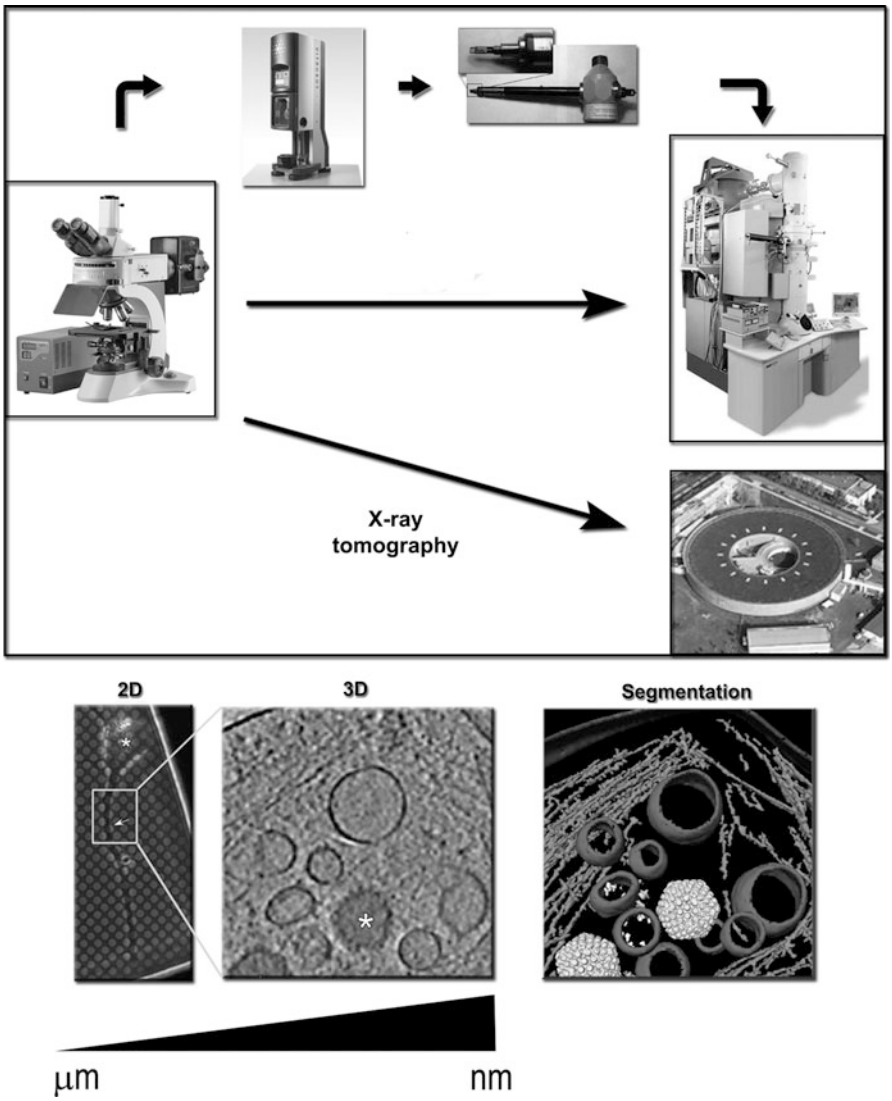

Fig. 7.8 Workflow in correlative microscopy. *Top*, Schematic of the methodological steps involved in performing correlative light and electron microscopy (CLEM). Cellular structures are sequentially identified with different microscopic techniques with increasing resolving power. Targeted processes in cells are imaged using a fluorescence microscope (*centre left*); then, the cells supported on a grid, are vitrified using a plunging freezing device (*top left*) and the grid transferred using a suitable cryo-holder (*top right*) in a field-emission-gun transmission electron microscope (*centre right*) for visualization of sub-cellular features by electron tomography; nowadays also X-ray tomography on entire cells can be performed at synchrotron facilities. *Bottom*, *left to right*: detection of the area of interest in 2D (using light microscopy; micrometer scale); visualization and 3D reconstruction by ET techniques (nanometer scale); segmentation of the different structural elements

The advent of correlative microscopy will benefit the study of those viruses that are characterized by low replication and infection efficiencies and have therefore escaped direct visualization. A clear example of this is hepatitis C virus, whose low-level replication *in vitro* has hampered the visualization of viral morphological processes by traditional ET technique.

7.7.2 Developing 3D Imaging Techniques

One of the most recent (and contentious) method developments in 3D image reconstruction algorithms that could, in principle, be used for initial low-resolution phasing is represented by ankylography [103]. Briefly, it consists in collecting on a curved detector the diffraction pattern generated by the scattering of a coherent soft X-ray laser hitting the object of interest (not necessarily crystalline). The proposed advantage of ankylography over XFEL crystallography or X-ray tomography is that, unlike these techniques, it uses a 2D spherical diffraction pattern to reconstruct the full 3D structure of the object. A proof-of-principle of this reconstruction method was the determination of poliovirus at 20–30 Å resolution [103]. So, while it might appear that ankylography might have an important impact, there is a fundamental problem in that capturing a thin spherical shell of data in reciprocal space is ultimately a very poor approximation to measuring the full 3D volume needed to produce a high resolution reconstruction [104].

As a variant on coherent X-ray scattering, ptychography, an imaging technique that was proposed in the late ‘60s by Hoppe [105] and aiming to solve the phase-problem by using an interference phenomenon has been recently re-emerging as an EM technique that could provide potentially superresolution (~5-Å) [106]. The principles behind ptychography have been also employed in X-ray tomography in life science experiments [107]. It will be interesting to see the ultimate scope of this method, however in its present form it is slow (even at a synchrotron) and requires a high radiation dose to achieve a 3D reconstruction at modest resolution.

7.8 The Biology Behind the Combined Methods

7.8.1 Implications for Drug-Design and Vaccine Development

Current methods for drug-discovery rely mainly on: (i) ligand-based design and (ii) structure-based design. In the first case the search for new compounds against a target molecule is based on previously known drugs; in the second case the search is based on the availability of the 3D structure of the target molecule (see Chap. 20 for a comprehensive view on the translational applications of structural virology

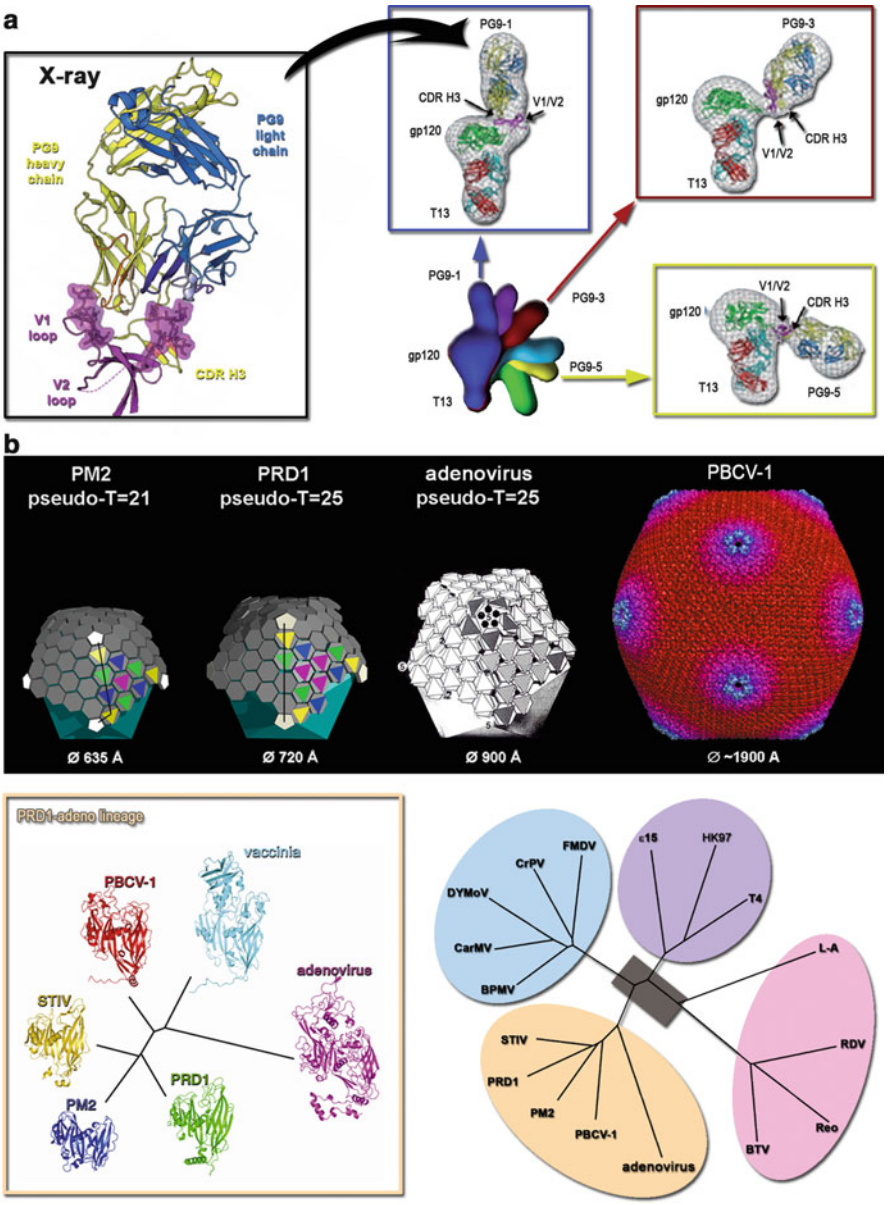

Fig. 7.9 Impact of the combination of structural methods. (**a**) *Left*, X-ray structure of the HIV-1 gp120 V1/V2 domain (in *magenta*) complexed with neutralizing antibody PG9 (*yellow*, heavy chain; *blue*, light-chain) represented as ribbons; *right*, negative stain EM reconstruction classes (six in total, colour-coded from *blue* to *green*) of ternary complexes composed by gp120, PG9 and CD4-binding-site antibody T13 with the corresponding fitting of the gp120 V1/V2-PG9 crystal structure in three of them (insets) (Adapted from [109]. With permission). (**b**) *Top left*, schematic representation of the architecture of bacteriophages PM2 and PRD1; *grey* hexagons represent the pseudo-hexameric morphology displayed by viral major capsid proteins forming trimers; the trimers composing the icosahedral asymmetric unit are represented as *colour-coded triangles*;

in antiviral research). Both screening strategies are computationally intensive. Structure-based design uses atomic or quasi atomic models to rationalize the interaction of the potential candidate drug with the target biomolecule, for example to block the binding of the virus to the cellular receptor. One of the first examples where the interdisciplinary approach of virus EM with X-ray crystallography has provided clues for the development of antiviral drugs is represented by the docking of ICAM I to human rhinovirus [26]. Indeed this quasi-atomic model (Fig. 7.3b) contributed to the development of pleconaril, a drug that inhibited the uncoating of rhinovirus upon infection by binding to the major capsid protein VP1 [108]. Although this drug was never licensed, failing in phase-clinic III studies [108], the whole process reinforced the utility of the combined approach in virus structure determination.

Undoubtedly, the interaction of viruses with their cellular receptors is one of the major structural targets in antiviral research facilitating the rational design of novel drugs aiming to halt cell entry. Similarly, studies aimed at understanding the mechanism of viral evasion of antibody neutralization, for example for HIV-1 gp120 [109], have made use of crystal structures and negative stain electron microscopy (Fig. 7.9a). Nevertheless there are other steps during virus morphogenesis that can be tackled by combining EM information and X-ray crystallography, for example targeting the ribonucleoprotein complex of influenza virus responsible for viral RNA synthesis [111]. Furthermore the structural elucidation of virus-like-particles (VLPs) as transporters of foreign antigenic epitopes (see Chap. 21) by combining cryo-EM and crystal structures of the component proteins allow the localization and investigation of the modifications introduced in the virus capsid structure. The knowledge of the conformation of the inserted epitope in the VLPs and their structural relationship with the rest of the particles directs possible improvements of construct design; examples include TBSV and Norovirus which have been used as a platform for polyvalent display of antigenic epitopes and vaccine design. Indeed structural virology has a huge potential for the structure-based development of next generation vaccines.

7.8.2 *Novel Concepts in Virus Evolution*

In the last decade the accumulation of virus and viral protein structures determined mainly by X-ray crystallography and cryo-EM or the combination of these two

Fig. 7.9 (continued) black-lines on the capsomers indicates the T numbers). *Top right*, adenovirus (Adapted from [3]), and the cryo-EM derived density of Paramecium bursaria chlorella virus-1 (PBCV-1) (image taken from http://viperdb.scripps.edu/info_page.php?VDB=1m4x). All four represented viruses are members of the PRD1-adeno viral lineage. *Bottom left*, structure-based phylogenetic tree of viral capsid protein members of the PRD1-adeno viral lineage (Reproduced from [110]. With permission). *Bottom right*, the four viral lineages so far grouped using the phylogenetic structural approach; each lineage includes some virus/phage representatives (PRD1-adeno viral lineage, *ocre*; BTV-like lineage, *pink*; Picorna-like lineage, *light-blue*; HK97-lineage, *violet*) (Reproduced with permission from Abrescia et al. 2010)

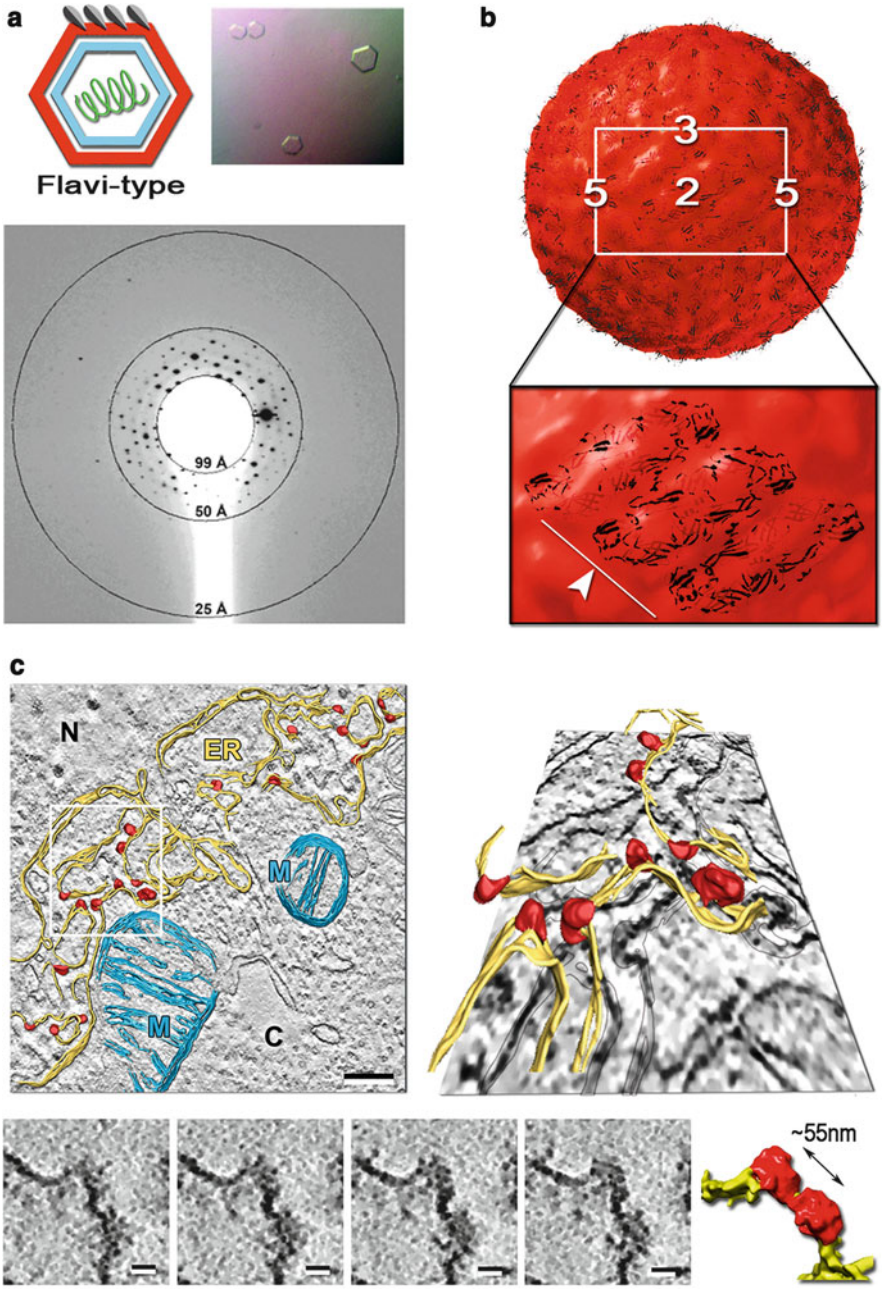

Fig. 7.10 Some of the challenges ahead. (**a**) *Top left*, scheme of a flavivirus; the envelope is shown in *red*, the glycoproteins in *grey* or *light-grey*, the capsid in *cyan* and the genomic RNA in *green*. *Top right*, one of the different morphologies of WNV crystals. *Bottom*, diffraction pattern at ~25-Å resolution corresponding to the crystals shown on top (Adapted from [113]. With permission). (**b**) *Top*, three-dimensional cryo-EM reconstruction of HCV-like-particles (HCV-LPs)

techniques has allowed us to look at the virus world (virosphere) on the basis of their structural relationships. This has led to the emergence of a novel concept in virus evolution that uses specific structural markers, the so-called virus-self elements (for example the fold of the capsid protein) to infer common ancestry [38]. Although the observation that viruses infecting different species (cf. SBMV vs. rhinovirus) displayed a similar structural fold in their capsid protein (single jelly-roll) goes back to 1985 [16], it was only in 2002 [38] that the capsid-centered view in virus classification was formalized as a precise hypothesis and through the years validated by the systematic experimental approach of structure comparisons [112]. This novel taxonomic approach allows us to simplify the organization of the virosphere and pinpoint relationships between viruses that infect different hosts across the three domains of life. A clear example of this is represented by adenovirus and PRD1, which infect vertebrate and bacteria, respectively. Their capsid proteins share a double jelly-roll fold and the capsids share common architectural principles [17] (Fig. 7.9b). The power of this structural classification is apparent in the fact that almost half of the virus families currently described, many of which do not belong to any order according to the International Committee on Taxonomy of Viruses (ICTV) classification scheme (see Chap. 1), can be traced back to one of the four viral lineages so far described: (*i*) PRD1/adenovirus-like, (*ii*) Blue-tongue-virus-like, (*iii*) HK97-like and (*iv*) Picorna-like [112] (Fig. 7.9b). It is unclear how many more virus lineages will be unveiled by the structure-based classification method since this depends on the discovery of new viral protein folds. Finally, this structure-based taxonomy of viruses opens the way to conceptualize anti-viral strategies that bridge viruses that were considered unrelated until now.

7.8.3 Perspectives and Challenges Ahead

Much progress has been made in the understanding virus biology thanks to the combination of biochemical, genetic and structural techniques. EM and X-ray crystallography have played (and still do) a dominant role in describing and

Fig. 7.10 (continued) (~500-Å in diameter) at 30-Å resolution; the icosahedral symmetry axes are indicated; *Bottom*, close-up of a HCV-LP capsid region; dengue virus glycoproteins (*black* cartoon models, indicated with a *white arrow-head* and *line*) have been fitted within the HCV-LP cryo-EM density (Adapted from [115]. With permission). (**c**) *Top*, electron tomographic reconstruction of Sf9 cells showing the cellular ER landscape when expressing hepatitis C virus-like-particles (HCV-LPs), and segmentation of its major structural elements. *Top left*, slice through the center of a denoised tomogram with superimposed rendering of the convoluted ER membranes in *gold*, budding HCV-LPs in *red* and mitochondria in *slate-blue*. Scale-bar = 200 nm. *Top right*, perspective view of the region outlined by a white rectangle. N = nucleus, C = cytoplasm, M = mitochondria, ER = endoplasmic reticulum. *Bottom*, four consecutive tomographic slices showing coalescence of HCV-LPs buds together with their isosurface representation and segmentation on the right. Scale-bar = 20 nm (Reproduced from [116]. With permission)

providing high-resolution viral structures, whilst their hybridization has provided insights into the mechanisms of virus-host recognition, antibody neutralization, antigen display, virus assembly and maturation and other properties and functions of virus particles (see Part III of this book, Chaps. 10, 11, 12, 13, 14, 15, 16, 17, 18 and 19). Nevertheless, efforts in the past have focused mainly on virus particles that display icosahedral morphology (about half the virus families known), which are easier to analyse, as described above.

Structural virology has still several challenges ahead, including the structural characterization at atomic resolution of enveloped viruses, such as members of the *Flaviviridae*, *Alphaviridae* and *Bunyaviridae* families, and even more complex viruses, such as the poxviruses.

Attempts to crystallize WNV, a member of the *Flaviviridae* family, have been carried out [113] and indeed crystals were obtained and diffracted to 25-Å resolution – not competitive with the 14-Å resolution achieved by cryo-EM [114] (Fig. 7.10a). Another structural challenge is the biomedically very important hepatitis C virus (HCV) whose architecture, structure of its glycoproteins and assembly are not understood. A wealth of biochemical information has been gathered on the HCV life-cycle in past and recent years but only very recently, have efforts focused on the structural characterization of the virus [115–117] (Fig. 7.10b).

Technological developments with synchrotron radiation with the advent of XFEL and the *in-situ* diffraction [118], or the routine use in EM of the phase-plate contrast technology [119], the new direct detection cameras and correlative microscopy will undoubtedly shape our investigation on virus structures in the near future.

To sum up, the hybridization of approaches in structural virology is a powerful method in generating knowledge and tools serving in the fight against viral infections. These contributions are fundamental to the health of humans and animals, and will help to create a "Systems Virology" vision capturing the complex biology of viruses.

Acknowledgements DB acknowledges support from the CIC bioGUNE and HMO thanks the University of Helsinki for funding to EU ESFRI Instruct Centre for Virus Production and Purification. DIS is supported by the UK MRC. This work was enabled by the Spanish Ministerio de Ciencia y Innovacion (BFU2009-08123), Spanish Ministerio de Economia y Competitividad (BFU2012-33947) and the Basque Government (PI2010-20) grants to NGAA.

References and Further Reading

1. Harrison SC, Olson AJ, Schutt CE, Winkler FK, Bricogne G (1978) Tomato bushy stunt virus at 2.9 Å resolution. Nature 276:368–373
2. Abad-Zapatero C, Abdel-Meguid SS, Johnson JE, Leslie AG, Rayment I, Rossmann MG, Suck D, Tsukihara T (1980) Structure of southern bean mosaic virus at 2.8Å resolution. Nature 286:33–39
3. Roberts MM, White JL, Grutter MG, Burnett RM (1986) Three-dimensional structure of the adenovirus major coat protein hexon. Science 232:1148–1151

4. Goldsmith CS, Miller SE (2009) Modern uses of electron microscopy for detection of viruses. Clin Microbiol Rev 22:552–563
5. Jiang W, Baker ML, Jakana J, Weigele PR, King J, Chiu W (2008) Backbone structure of the infectious epsilon15 virus capsid revealed by electron cryomicroscopy. Nature 451:1130–1134
6. Hagen C, Guttmann P, Klupp B, Werner S, Rehbein S, Mettenleiter TC, Schneider G, Grünewald K (2012) Correlative VIS-fluorescence and soft X-ray cryo-microscopy/tomography of adherent cells. J Struct Biol 177:193–201
7. Svergun DI, Koch MH (2003) Small-angle scattering studies of biological macromolecules in solution. Rep Prog Phys 66:1735–1782
8. Svergun DI, Koch MH (2002) Advances in structure analysis using small-angle scattering in solution. Curr Opin Struct Biol 12:654–660
9. Stubbs G (2001) Fibre diffraction studies of filamentous viruses. Rep Prog Phys 64:1389–1425
10. Harrison SC, Caspar DL, Camerini-Otero RD, Franklin RM (1971) Lipid and protein arrangement in bacteriophage PM2. Nat New Biol 229:197–201
11. Abrescia NG, Grimes JM, Kivela HM, Assenberg R, Sutton GC, Butcher SJ, Bamford JK, Bamford DH, Stuart DI (2008) Insights into virus evolution and membrane biogenesis from the structure of the marine lipid-containing bacteriophage PM2. Mol Cell 31:749–761
12. Canady MA, Tsuruta H, Johnson JE (2001) Analysis of rapid, large-scale protein quaternary structural changes: time-resolved X-ray solution scattering of Nudaurelia capensis omega virus (NomegaV) maturation. J Mol Biol 311:803–814
13. Fry EE, Abrescia NGA, Stuart DI (2007) Virus crystallography. In: Sanderson M, Skelly J (eds) Macromolecular crystallography: conventional and high-throughput methods – a practical approach. Oxford University Press, Oxford
14. Tuthill TJ, Harlos K, Walter TS, Knowles NJ, Groppelli E, Rowlands DJ, Stuart DI, Fry EE (2009) Equine rhinitis A virus and its low pH empty particle: clues towards an aphthovirus entry mechanism? PLoS Pathog 5:e1000620
15. Hogle JM, Chow M, Filman DJ (1985) Three-dimensional structure of poliovirus at 2.9 A resolution. Science 229:1358–1365
16. Rossmann MG, Arnold E, Erickson JW, Frankenberger EA, Griffith JP, Hecht H, Johnson JJ, Kamer G, Luo M, Mosser AG, Rueckert RR, Sherry B, Vriend G (1985) Structure of a human common cold virus and functional relationship to other picornaviruses. Nature 317:145–153
17. Abrescia NG, Cockburn JJ, Grimes JM, Sutton GC, Diprose JM, Butcher SJ, Fuller SD, San Martín C, Burnett RM, Stuart DI, Bamford DH, Bamford JK (2004) Insights into assembly from structural analysis of bacteriophage PRD1. Nature 432:68–74
18. Cockburn JJ, Abrescia NG, Grimes JM, Sutton GC, Diprose JM, Benevides JM, Thomas GJ Jr, Bamford JK, Bamford DH, Stuart DI (2004) Membrane structure and interactions with protein and DNA in bacteriophage PRD1. Nature 432:122–125
19. Liu H, Jin L, Koh SB, Atanasov I, Schein S, Wu L, Zhou ZH (2010) Atomic structure of human adenovirus by cryo-EM reveals interactions among protein networks. Science 329:1038–1043
20. Reddy VS, Natchiar SK, Stewart PL, Nemerow GR (2010) Crystal structure of human adenovirus at 3.5 A resolution. Science 329:1071–1075
21. Perrakis A, Daenke S, Stuart DI, Sussman JL (2011) From SPINE to SPINE-2 complexes and beyond. J Struct Biol 175:105
22. Axford D, Owen RL, Aishima J, Foadi J, Morgan AW, Robinson JI, Nettleship JE, Owens RJ, Moraes I, Fry EE, Grimes JM, Harlos K, Kotecha A, Ren J, Sutton G, Walter TS, Stuart DI, Evans G (2012) In situ macromolecular crystallography using microbeams. Acta Crystallogr D Biol Crystallogr 68:592–600
23. Wang X, Peng W, Ren J, Hu Z, Xu J, Lou Z, Li X, Yin W, Shen X, Porta C, Walter TS, Evans G, Axford D, Owen R, Rowlands DJ, Wang J, Stuart DI, Fry EE, Rao Z (2012) A sensor-

adaptor mechanism for enterovirus uncoating from structures of EV71. Nat Struct Mol Biol 19:424–429
24. Evans G, Axford D, Owen RL (2011) The design of macromolecular crystallography diffraction experiments. Acta Crystallogr D Biol Crystallogr 67:261–270
25. Rossmann MG (2000) Fitting atomic models into electron-microscopy maps. Acta Crystallogr D Biol Crystallogr 56:1341–1349
26. Kolatkar PR, Bella J, Olson NH, Bator CM, Baker TS, Rossmann MG (1999) Structural studies of two rhinovirus serotypes complexed with fragments of their cellular receptor. EMBO J 18:6249–6259
27. Gilbert RJ, Grimes JM, Stuart DI (2003) Hybrid vigor: hybrid methods in viral structure determination. Adv Protein Chem 64:37–91
28. Topf M, Sali A (2005) Combining electron microscopy and comparative protein structure modeling. Curr Opin Struct Biol 15:578–585
29. Kaufmann KW, Lemmon GH, Deluca SL, Sheehan JH, Meiler J (2010) Practically useful: what the Rosetta protein modeling suite can do for you. Biochemistry 49:2987–2998
30. Franklin RE, Harrison SC, Pettersson U, Philipson L, Branden CJ, Werner P (1971) Structural studies on the adenovirus hexon. Cold Spring Harb Symp Quant Biol 36:503–510
31. Hewat EA, Verdaguer N, Fita I, Blakemore W, Brookes S, King A, Newman J, Domingo E, Mateu MG, Stuart DI (1997) Structure of the complex of an Fab fragment of a neutralizing antibody with foot-and-mouth disease virus: positioning of a highly mobile antigenic loop. EMBO J 16:1492–1500
32. Yu IM, Zhang W, Holdaway HA, Li L, Kostyuchenko VA, Chipman PR, Kuhn RJ, Rossmann MG, Chen J (2008) Structure of the immature dengue virus at low pH primes proteolytic maturation. Science 319:1834–1837
33. Li L, Lok SM, Yu IM, Zhang Y, Kuhn RJ, Chen J, Rossmann MG (2008) The flavivirus precursor membrane-envelope protein complex: structure and maturation. Science 319:1830–1834
34. Cherrier MV, Kaufmann B, Nybakken GE, Lok SM, Warren JT, Chen BR, Nelson CA, Kostyuchenko VA, Holdaway HA, Chipman PR, Kuhn RJ, Diamond MS, Rossmann MG, Fremont DH (2009) Structural basis for the preferential recognition of immature flaviviruses by a fusion-loop antibody. EMBO J 28:3269–3276
35. Bamford DH, Caldentey J, Bamford JK (1995) Bacteriophage PRD1: a broad host range dsDNA tectivirus with an internal membrane. Adv Virus Res 45:281–319
36. San Martin C, Burnett RM, de Haas F, Heinkel R, Rutten T, Fuller SD, Butcher SJ, Bamford DH (2001) Combined EM/X-Ray imaging yields a quasi-atomic model of the adenovirus-related bacteriophage PRD1 and shows key capsid and membrane interactions. Structure 9:917–930
37. Benson SD, Bamford JK, Bamford DH, Burnett RM (1999) Viral evolution revealed by bacteriophage PRD1 and human adenovirus coat protein structures. Cell 98:825–833
38. Bamford DH, Burnett RM, Stuart DI (2002) Evolution of viral structure. Theor Popul Biol 61:461–470
39. Nickell S, Forster F, Linaroudis A, Net WD, Beck F, Hegerl R, Baumeister W, Plitzko JM (2005) TOM software toolbox: acquisition and analysis for electron tomography. J Struct Biol 149:227–234
40. Scheres SH, Melero R, Valle M, Carazo JM (2009) Averaging of electron subtomograms and random conical tilt reconstructions through likelihood optimization. Structure 17:1563–1572
41. Castaño-Diez D, Kudryashev M, Arheit M, Stahlberg H (2012) Dynamo: a flexible, user-friendly development tool for subtomogram averaging of cryo-EM data in high-performance computing environments. J Struct Biol 178:139–151
42. Briggs JA, Riches JD, Glass B, Bartonova V, Zanetti G, Kräusslich HG (2009) Structure and assembly of immature HIV. Proc Natl Acad Sci U S A 106:11090–11095

43. Alber F, Dokudovskaya S, Veenhoff LM, Zhang W, Kipper J, Devos D, Suprapto A, Karni-Schmidt O, Williams R, Chait BT, Sali A, Rout MP (2007) The molecular architecture of the nuclear pore complex. Nature 450:695–701
44. Brunger AT (1992) Free R value: a novel statistical quantity for assessing the accuracy of crystal structures. Nature 355:472–475
45. Tsao J, Chapman MS, Rossmann MG (1992) Ab initio phase determination for viruses with high symmetry: a feasibility study. Acta Crystallogr A 48(Pt 3):293–301
46. Chapman MS, Tsao J, Rossmann MG (1992) Ab initio phase determination for spherical viruses: parameter determination for spherical-shell models. Acta Crystallogr A 48(Pt 3): 301–312
47. Rossmann MG (1995) Ab initio phase determination and phase extension using non-crystallographic symmetry. Curr Opin Struct Biol 5:650–655
48. Rossmann MG (1990) The molecular replacement method. Acta Crystallogr A 46(Pt 2):73–82
49. Acharya R, Fry E, Stuart D, Fox G, Rowlands D, Brown F (1989) The three-dimensional structure of foot-and-mouth disease virus at 2.9 Å resolution. Nature 337:709–716
50. Villeret V, Tricot C, Stalon V, Dideberg O (1995) Crystal structure of Pseudomonas aeruginosa catabolic ornithine transcarbamoylase at 3.0 Å resolution: a different oligomeric organization in the transcarbamoylase family. Proc Natl Acad Sci U S A 92:10762–10766
51. Dodson EJ (2001) Using electron-microscopy images as a model for molecular replacement. Acta Crystallogr D Biol Crystallogr 57:1405–1409
52. Navaza J (2008) Combining X-ray and electron-microscopy data to solve crystal structures. Acta Crystallogr D Biol Crystallogr 64:70–75
53. Trapani S, Schoehn G, Navaza J, Abergel C (2010) Macromolecular crystal data phased by negative-stained electron-microscopy reconstructions. Acta Crystallogr D Biol Crystallogr 66:514–521
54. Hao Q, Dodd FE, Grossmann JG, Hasnain SS (1999) Ab initio phasing using molecular envelope from solution X-ray scattering. Acta Crystallogr D Biol Crystallogr 55:243–246
55. Huiskonen JT, Kivelä HM, Bamford DH, Butcher SJ (2004) The PM2 virion has a novel organization with an internal membrane and pentameric receptor binding spikes. Nat Struct Mol Biol 11:850–856
56. Abrescia NG, Grimes JM, Oksanen HM, Bamford JK, Bamford DH, Stuart DI (2011) The use of low-resolution phasing followed by phase extension from 7.6 to 2.5 Å resolution with noncrystallographic symmetry to solve the structure of a bacteriophage capsid protein. Acta Crystallogr D Biol Crystallogr 67:228–232
57. Abrescia NG, Kivelä HM, Grimes JM, Bamford JK, Bamford DH, Stuart DI (2005) Preliminary crystallographic analysis of the major capsid protein P2 of the lipid-containing bacteriophage PM2. Acta Crystallogr Sect F Struct Biol Cryst Commun 61:762–765
58. Leitner A, Reischl R, Walzthoeni T, Herzog F, Bohn S, Förster F, Aebersold R (2012) Expanding the chemical cross-linking toolbox by the use of multiple proteases and enrichment by size exclusion chromatography. Mol Cell Proteomics 11(M111):014126
59. Gowen B, Bamford JK, Bamford DH, Fuller SD (2003) The tailless icosahedral membrane virus PRD1 localizes the proteins involved in genome packaging and injection at a unique vertex. J Virol 77:7863–7871
60. Strömsten NJ, Bamford DH, Bamford JK (2003) The unique vertex of bacterial virus PRD1 is connected to the viral internal membrane. J Virol 77:6314–6321
61. Kivelä HM, Madonna S, Krupovic M, Tutino ML, Bamford JK (2008) Genetics for Pseudoalteromonas provides tools to manipulate marine bacterial virus PM2. J Bacteriol 190:1298–1307
62. Avilov SV, Moisy D, Munier S, Schraidt O, Naffakh N, Cusack S (2011) Replication-competent influenza A virus that encodes a split-green fluorescent protein-tagged PB2 polymerase subunit allows live-cell imaging of the virus life cycle. J Virol 86:1433–1448

63. Kivelä HM, Abrescia NG, Bamford JK, Grimes JM, Stuart DI, Bamford DH (2008) Selenomethionine labeling of large biological macromolecular complexes: probing the structure of marine bacterial virus PM2. J Struct Biol 161:204–210
64. Bamford D, Mindich L (1982) Structure of the lipid-containing bacteriophage PRD1: disruption of wild-type and nonsense mutant phage particles with guanidine hydrochloride. J Virol 44:1031–1038
65. Kivelä HM, Kalkkinen N, Bamford DH (2002) Bacteriophage PM2 has a protein capsid surrounding a spherical proteinaceous lipid core. J Virol 76:8169–8178
66. Caldentey J, Luo C, Bamford DH (1993) Dissociation of the lipid-containing bacteriophage PRD1: effects of heat, pH, and sodium dodecyl sulfate. Virology 194:557–563
67. Kivelä HM, Roine E, Kukkaro P, Laurinavicius S, Somerharju P, Bamford DH (2006) Quantitative dissociation of archaeal virus SH1 reveals distinct capsid proteins and a lipid core. Virology 356:4–11
68. Pietilä MK, Atanasova NS, Manole V, Liljeroos L, Butcher SJ, Oksanen HM, Bamford DH (2012) Virion architecture unifies globally distributed pleolipoviruses infecting halophilic archaea. J Virol 86:5067–5079
69. Rissanen I, Pawlowski A, Harlos K, Grimes JM, Stuart DI, Bamford JKH (2012) Crystallization and preliminary crystallographic analysis of the major capsid proteins VP16 and VP17 of bacteriophage P23-77. Acta Crystallogr F68:580–583
70. Aricescu AR, Lu W, Jones EY (2006) A time- and cost-efficient system for high-level protein production in mammalian cells. Acta Crystallogr D Biol Crystallogr 62:1243–1250
71. Benson SD, Bamford JK, Bamford DH, Burnett RM (2002) The X-ray crystal structure of P3, the major coat protein of the lipid-containing bacteriophage PRD1, at 1.65 A resolution. Acta Crystallogr D Biol Crystallogr 58:39–59
72. Hendrickson WA (1991) Determination of macromolecular structures from anomalous diffraction of synchrotron radiation. Science 254:51–58
73. Jeembaeva M, Jonsson B, Castelnovo M, Evilevitch A (2010) DNA heats up: energetics of genome ejection from phage revealed by isothermal titration calorimetry. J Mol Biol 395:1079–1087
74. Walter TS, Ren J, Tuthill TJ, Rowlands DJ, Stuart DI, Fry EE (2012) A plate-based high throughput assay for virus stability and vaccine formulation. J Virol Methods 185(1):166–170
75. Shoemaker GK, van Duijn E, Crawford SE, Uetrecht C, Baclayon M, Roos WH, Wuite GJ, Estes MK, Prasad BV, Heck AJ (2010) Norwalk virus assembly and stability monitored by mass spectrometry. Mol Cell Proteomics 9:1742–1751
76. Lucic V, Forster F, Baumeister W (2005) Structural studies by electron tomography: from cells to molecules. Annu Rev Biochem 74:833–865
77. Subramaniam S, Bartesaghi A, Liu J, Bennett AE, Sougrat R (2007) Electron tomography of viruses. Curr Opin Struct Biol 17:596–602
78. Freiberg AN, Sherman MB, Morais MC, Holbrook MR, Watowich SJ (2008) Three-dimensional organization of Rift Valley fever virus revealed by cryoelectron tomography. J Virol 82:10341–10348
79. Grünewald K, Desai P, Winkler DC, Heymann JB, Belnap DM, Baumeister W, Steven AC (2003) Three-dimensional structure of herpes simplex virus from cryo-electron tomography. Science 302:1396–1398
80. Bowman BR, Baker ML, Rixon FJ, Chiu W, Quiocho FA (2003) Structure of the herpesvirus major capsid protein. EMBO J 22:757–765
81. Baker ML, Jiang W, Rixon FJ, Chiu W (2005) Common ancestry of herpesviruses and tailed DNA bacteriophages. J Virol 79:14967–14970
82. Bostina M, Bubeck D, Schwartz C, Nicastro D, Filman DJ, Hogle JM (2007) Single particle cryoelectron tomography characterization of the structure and structural variability of poliovirus-receptor-membrane complex at 30 A resolution. J Struct Biol 160:200–210
83. Zhu P, Liu J, Bess J Jr, Chertova E, Lifson JD, Grisé H, Ofek GA, Taylor KA, Roux KH (2006) Distribution and three-dimensional structure of AIDS virus envelope spikes. Nature 441:847–852

84. Zanetti G, Briggs JA, Grünewald K, Sattentau QJ, Fuller SD (2006) Cryo-electron tomographic structure of an immunodeficiency virus envelope complex in situ. PLoS Pathog 2:e83
85. Chen B, Vogan EM, Gong H, Skehel JJ, Wiley DC, Harrison SC (2005) Structure of an unliganded simian immunodeficiency virus gp120 core. Nature 433:834–841
86. Liu J, Bartesaghi A, Borgnia MJ, Sapiro G, Subramaniam S (2008) Molecular architecture of native HIV-1 gp120 trimers. Nature 455:109–113
87. Harris A, Cardone G, Winkler DC, Heymann JB, Brecher M, White JM, Steven AC (2006) Influenza virus pleiomorphy characterized by cryoelectron tomography. Proc Natl Acad Sci U S A 103:19123–19127
88. Huiskonen JT, Overby AK, Weber F, Grünewald K (2009) Electron cryo-microscopy and single-particle averaging of Rift Valley fever virus: evidence for GN-GC glycoprotein heterodimers. J Virol 83:3762–3769
89. Carrascosa JL, Chichon FJ, Pereiro E, Rodriguez MJ, Fernandez JJ, Esteban M, Heim S, Guttmann P, Schneider G (2009) Cryo-X-ray tomography of vaccinia virus membranes and inner compartments. J Struct Biol 168:234–239
90. Ji X, Sutton G, Evans G, Axford D, Owen R, Stuart DI (2009) How baculovirus polyhedra fit square pegs into round holes to robustly package viruses. EMBO J 29:505–514
91. Koopmann R, Cupelli K, Redecke L, Nass K, Deponte DP, White TA, Stellato F, Rehders D, Liang M, Andreasson J, Aquila A, Bajt S, Barthelmess M, Barty A, Bogan MJ, Bostedt C, Boutet S, Bozek JD, Caleman C, Coppola N, Davidsson J, Doak RB, Ekeberg T, Epp SW, Erk B, Fleckenstein H, Foucar L, Graafsma H, Gumprecht L, Hajdu J, Hampton CY, Hartmann A, Hartmann R, Hauser G, Hirsemann H, Holl P, Hunter MS, Kassemeyer S, Kirian RA, Lomb L, Maia FR, Kimmel N, Martin AV, Messerschmidt M, Reich C, Rolles D, Rudek B, Rudenko A, Schlichting I, Schulz J, Seibert MM, Shoeman RL, Sierra RG, Soltau H, Stern S, Strüder L, Timneanu N, Ullrich J, Wang X, Weidenspointner G, Weierstall U, Williams GJ, Wunderer CB, Fromme P, Spence JC, Stehle T, Chapman HN, Betzel C, Duszenko M (2012) *In vivo* protein crystallization opens new routes in structural biology. Nat Methods 9:259–262
92. Iwasaki K, Omura T (2010) Electron tomography of the supramolecular structure of virus-infected cells. Curr Opin Struct Biol 20:632–639
93. Chapman HN, Fromme P, Barty A, White TA, Kirian RA, Aquila A, Hunter MS, Schulz J, DePonte DP, Weierstall U, Doak RB, Maia FR, Martin AV, Schlichting I, Lomb L, Coppola N, Shoeman RL, Epp SW, Hartmann R, Rolles D, Rudenko A, Foucar L, Kimmel N, Weidenspointner G, Holl P, Liang M, Barthelmess M, Caleman C, Boutet S, Bogan MJ, Krzywinski J, Bostedt C, Bajt S, Gumprecht L, Rudek B, Erk B, Schmidt C, Hömke A, Reich C, Pietschner D, Strüder L, Hauser G, Gorke H, Ullrich J, Herrmann S, Schaller G, Schopper F, Soltau H, Kühnel KU, Messerschmidt M, Bozek JD, Hau-Riege SP, Frank M, Hampton CY, Sierra RG, Starodub D, Williams GJ, Hajdu J, Timneanu N, Seibert MM, Andreasson J, Rocker A, Jönsson O, Svenda M, Stern S, Nass K, Andritschke R, Schröter CD, Krasniqi F, Bott M, Schmidt KE, Wang X, Grotjohann I, Holton JM, Barends TR, Neutze R, Marchesini S, Fromme R, Schorb S, Rupp D, Adolph M, Gorkhover T, Andersson I, Hirsemann H, Potdevin G, Graafsma H, Nilsson B, Spence JC (2011) Femtosecond X-ray protein nanocrystallography. Nature 470:73–77
94. Seibert MM, Ekeberg T, Maia FR, Svenda M, Andreasson J, Jönsson O, Odić D, Iwan B, Rocker A, Westphal D, Hantke M, DePonte DP, Barty A, Schulz J, Gumprecht L, Coppola N, Aquila A, Liang M, White TA, Martin A, Caleman C, Stern S, Abergel C, Seltzer V, Claverie JM, Bostedt C, Bozek JD, Boutet S, Miahnahri AA, Messerschmidt M, Krzywinski J, Williams G, Hodgson KO, Bogan MJ, Hampton CY, Sierra RG, Starodub D, Andersson I, Bajt S, Barthelmess M, Spence JC, Fromme P, Weierstall U, Kirian R, Hunter M, Doak RB, Marchesini S, Hau-Riege SP, Frank M, Shoeman RL, Lomb L, Epp SW, Hartmann R, Rolles D, Rudenko A, Schmidt C, Foucar L, Kimmel N, Holl P, Rudek B, Erk B, Hömke A, Reich C, Pietschner D, Weidenspointner G, Strüder L, Hauser G, Gorke H, Ullrich J, Schlichting I, Herrmann S, Schaller G, Schopper F, Soltau H, Kühnel KU, Andritschke R, Schröter CD,

Krasniqi F, Bott M, Schorb S, Rupp D, Adolph M, Gorkhover T, Hirsemann H, Potdevin G, Graafsma H, Nilsson B, Chapman HN, Hajdu J (2011) Single mimivirus particles intercepted and imaged with an X-ray laser. Nature 470:78–81
95. Lebbink MN, Geerts WJ, van der Krift TP, Bouwhuis M, Hertzberger LO, Verkleij AJ, Koster AJ (2007) Template matching as a tool for annotation of tomograms of stained biological structures. J Struct Biol 158:327–335
96. Pintilie GD, Zhang J, Goddard TD, Chiu W, Gossard DC (2010) Quantitative analysis of cryo-EM density map segmentation by watershed and scale-space filtering, and fitting of structures by alignment to regions. J Struct Biol 170:427–438
97. Liljeroos L, Huiskonen JT, Ora A, Susi P, Butcher SJ (2011) Electron cryotomography of measles virus reveals how matrix protein coats the ribonucleocapsid within intact virions. Proc Natl Acad Sci U S A 108:18085–18090
98. Brandt F, Carlson LA, Hartl FU, Baumeister W, Grünewald K (2010) The three-dimensional organization of polyribosomes in intact human cells. Mol Cell 39:560–569
99. Plitzko JM, Rigort A, Leis A (2009) Correlative cryo-light microscopy and cryo-electron tomography: from cellular territories to molecular landscapes. Curr Opin Biotechnol 20:83–89
100. van Driel LF, Valentijn JA, Valentijn KM, Koning RI, Koster AJ (2009) Tools for correlative cryo-fluorescence microscopy and cryo-electron tomography applied to whole mitochondria in human endothelial cells. Eur J Cell Biol 88:669–684
101. Kukulski W, Schorb M, Welsch S, Picco A, Kaksonen M, Briggs JA (2011) Correlated fluorescence and 3D electron microscopy with high sensitivity and spatial precision. J Cell Biol 192:111–119
102. Jun S, Ke D, Debiec K, Zhao G, Meng X, Ambrose Z, Gibson GA, Watkins SC, Zhang P (2011) Direct visualization of HIV-1 with correlative live-cell microscopy and cryo-electron tomography. Structure 19:1573–1581
103. Raines KS, Salha S, Sandberg RL, Jiang H, Rodriguez JA, Fahimian BP, Kapteyn HC, Du J, Miao J (2010) Three-dimensional structure determination from a single view. Nature 463:214–217
104. Reich ES (2011) Three-dimensional technique on trial. Nature 480:303
105. Hoppe W, Langer R, Frank J, Feltynowski A (1969) Image differentiation procedures in electron microscopy. Naturwissenschaften 56:267–272
106. Maiden AM, Humphry MJ, Zhang F, Rodenburg JM (2011) Superresolution imaging *via* ptychography. J Opt Soc Am A Opt Image Sci Vis 28:604–612
107. Dierolf M, Menzel A, Thibault P, Schneider P, Kewish CM, Wepf R, Bunk O, Pfeiffer F (2010) Ptychographic X-ray computed tomography at the nanoscale. Nature 467:436–439
108. Rossmann MG (2012) Crystallography, evolution, and the structure of viruses. J Biol Chem 287:9552–9559
109. McLellan JS, Pancera M, Carrico C, Gorman J, Julien JP, Khayat R, Louder R, Pejchal R, Sastry M, Dai K, O'Dell S, Patel N, Shahzad-ul-Hussan S, Yang Y, Zhang B, Zhou T, Zhu J, Boyington JC, Chuang GY, Diwanji D, Georgiev I, Kwon YD, Lee D, Louder MK, Moquin S, Schmidt SD, Yang ZY, Bonsignori M, Crump JA, Kapiga SH, Sam NE, Haynes BF, Burton DR, Koff WC, Walker LM, Phogat S, Wyatt R, Orwenyo J, Wang LX, Arthos J, Bewley CA, Mascola JR, Nabel GJ, Schief WR, Ward AB, Wilson IA, Kwong PD (2011) Structure of HIV-1 gp120 V1/V2 domain with broadly neutralizing antibody PG9. Nature 480:336–343
110. Bahar MW, Graham SC, Stuart DI, Grimes JM (2011) Insights into the evolution of a complex virus from the crystal structure of vaccinia virus d13. Structure 19:1011–1020
111. Coloma R, Valpuesta JM, Arranz R, Carrascosa JL, Ortin J, Martín-Benito J (2009) The structure of a biologically active influenza virus ribonucleoprotein complex. PLoS Pathog 5: e1000491
112. Abrescia NG, Bamford DH, Grimes JM, Stuart DI (2012) Structure unifies the viral universe. Annu Rev Biochem 81:795–822

113. Kaufmann B, Plevka P, Kuhn RJ, Rossmann MG (2010) Crystallization and preliminary X-ray diffraction analysis of West Nile virus. Acta Crystallogr Sect F Struct Biol Cryst Commun 66:558–562
114. Kaufmann B, Nybakken GE, Chipman PR, Zhang W, Diamond MS, Fremont DH, Kuhn RJ, Rossmann MG (2006) West Nile virus in complex with the Fab fragment of a neutralizing monoclonal antibody. Proc Natl Acad Sci U S A 103:12400–12404
115. Yu X, Qiao M, Atanasov I, Hu Z, Kato T, Liang TJ, Zhou ZH (2007) Cryo-electron microscopy and three-dimensional reconstructions of hepatitis C virus particles. Virology 367:126–134
116. Badia-Martinez D, Peralta B, Andrés G, Guerra M, Gil-Carton D, Abrescia NG (2012) Three-dimensional visualization of forming Hepatitis C virus-like particles by electron-tomography. Virology 430:120–126
117. Gastaminza P, Dryden KA, Boyd B, Wood MR, Law M, Yeager M, Chisari FV (2010) Ultrastructural and biophysical characterization of hepatitis C virus particles produced in cell culture. J Virol 84:10999–11009
118. Owen RL, Axford D, Nettleship JE, Owens RJ, Robinson JI, Morgan AW, Doré AS, Lebon G, Tate CG, Fry EE, Ren J, Stuart DI, Evans G (2012) Outrunning free radicals in room-temperature macromolecular crystallography. Acta Crystallogr D Biol Crystallogr 68:810–818
119. Murata K, Liu X, Danev R, Jakana J, Schmid MF, King J, Nagayama K, Chiu W (2010) Zernike phase contrast cryo-electron microscopy and tomography for structure determination at nanometer and subnanometer resolutions. Structure 18:903–912

Further Reading

Abeyrathne PD, Chami M, Pantelic RS, Goldie KN, Stahlberg H (2010) Preparation of 2D crystals of membrane proteins for high-resolution electron crystallography data collection. Methods Enzymol 481:25–43

Abrescia NG, Grimes JM, Fry EE, Ravantti JJ, Bamford DH, Stuart DI (2010) What does it take to make a virus: the concept of the viral "self". In: Twarock R, Stockley PG (eds) Emerging topics in physical virology. Imperial College Press, London, pp 35–58

Derosier D (2010) 3D reconstruction from electron micrographs a personal account of its development. Methods Enzymol 481:1–24

Henderson R, Sali A, Baker ML, Carragher B, Devkota B, Downing KH, Egelman EH, Feng Z, Frank J, Grigorieff N, Jiang W, Ludtke SJ, Medalia O, Penczek PA, Rosenthal PB, Rossmann MG, Schmid MF, Schröder GF, Steven AC, Stokes DL, Westbrook JD, Wriggers W, Yang H, Young J, Berman HM, Chiu W, Kleywegt GJ, Lawson CL (2012) Outcome of the first electron microscopy validation task force meeting. Structure 20:205–214

Johnson JE (2008) Multi-disciplinary studies of viruses: the role of structure in shaping the questions and answers. J Struct Biol 163:246–253

Perutz MF, Rossmann MG, Cullis AF, Muirhead H, Will G, North AC (1960) Structure of haemoglobin: a three-dimensional Fourier synthesis at 5.5-A. Resolution, obtained by X-ray analysis. Nature 185:416–422

Putnam CD, Hammel M, Hura GL, Tainer JA (2007) X-ray solution scattering (SAXS) combined with crystallography and computation: defining accurate macromolecular structures, conformations and assemblies in solution. Q Rev Biophys 40:191–285

Read RJ, Adams PD, Arendall WB III, Brunger AT, Emsley P, Joosten RP, Kleywegt GJ, Krissinel EB, Lütteke T, Otwinowski Z, Perrakis A, Richardson JS, Sheffler WH, Smith JL, Tickle IJ, Vriend G, Zwart PH (2011) A new generation of crystallographic validation tools for the protein data bank. Structure 19:1395–1412

Steven AC, Baumeister W (2008) The future is hybrid. J Struct Biol 163:186–195
Vellieux FM, Read RJ (1997) Noncrystallographic symmetry averaging in phase refinement and extension. Methods Enzymol 277:18–53

Also especially recommended for further reading are references [7, 9, 13, 25, 27, 99, 112] *listed above*.